

การเร่งการเจริญเติบโตของจุลสาหร่ายด้วยการเปลี่ยนรูปคาร์บอนไดออกไซด์



นายยศสวัสดิ์ พิเชียรสุนทร

ศูนย์วิทยทรัพยากร

วิทยานิพนธ์นี้เป็นส่วนหนึ่งของการศึกษาตามหลักสูตรปริญญาวิศวกรรมศาสตรมหาบัณฑิต

สาขาวิชาวิศวกรรมเคมี ภาควิชาวิศวกรรมเคมี

คณะวิศวกรรมศาสตร์ จุฬาลงกรณ์มหาวิทยาลัย

ปีการศึกษา 2553

ลิขสิทธิ์ของจุฬาลงกรณ์มหาวิทยาลัย



ACCELERATING MICROALGAL GROWTH
WITH CO₂ TRANSFORMATION

Mr. Yossaran Pichiansoontorn

A Thesis Submitted in Partial Fulfillment of the Requirements
for the Degree of Master of Engineering Program in Chemical Engineering

Department of Chemical Engineering

Faculty of Engineering

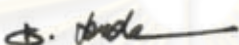
Chulalongkorn University

Academic Year 2010

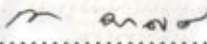
Copyright of Chulalongkorn University

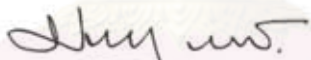
Thesis Title ACCELERATING MICROALGAL GROWTH
WITH CO₂ TRANSFORMATION
By Mr. Yossaran Pichainsoontorn
Field of Study Chemical Engineering
Thesis Advisor Associate Professor Prasert Pavasant, Ph.D.


Accepted by the Faculty of Engineering, Chulalongkorn University in
Partial Fulfillment of the Requirements for the Master's Degree


..... Dean of the Faculty of Engineering
(Associate Professor Boonsom Lerdkhironwong, Dr.Ing.)

THESIS COMMITTEE


..... Chairman
(Associate Professor Tharathon Mongkhonsi, Ph.D.)


..... Thesis Advisor
(Associate Professor Prasert Pavasant, Ph.D.)


..... Examiner
(Jirdsak Tscheikuna, Ph.D.)


..... External Examiner
(Associate Professor Tawan Sooknoi, Ph.D.)

ยศสวัสดิ์ พิเชียรสุนทร: การเร่งการเจริญเติบโตของจุลสาหร่ายด้วยการเปลี่ยนรูปคาร์บอนไดออกไซด์. (ACCELERATING MICROALGAL GROWTH WITH CO₂ TRANSFORMATION) อ.ที่ปรึกษาวิทยานิพนธ์หลัก: รศ.ดร. ประเสริฐ ภาวนันต์, 99 หน้า.

การเพิ่มประสิทธิภาพในการดักจับแก๊สคาร์บอนไดออกไซด์ในน้ำเพื่อเป็นแหล่งคาร์บอนอินทรีย์สำหรับการเร่งการเจริญเติบโตของจุลสาหร่ายได้ถูกศึกษาโดยผลของค่าพีเอช, พื้นที่สัมผัสสำหรับแก๊สและของเหลว, ความสูง, อัตราการไหลของแก๊ส และความเค็มของน้ำทะเล ที่มีผลต่อความเข้มข้นของคาร์บอนอินทรีย์โดยรวมที่ละลายน้ำได้นำมาศึกษา การทดลองได้ถูกกระทำขึ้นที่หอป้อนอากาศและหอที่มีวัสดุแพคที่มีความสูง 1-3 เมตร ค่าพีเอชของน้ำที่ทำการกำจัดแร่ธาตุออกได้ถูกปรับโดยใช้สารละลายโซเดียมไฮดรอกไซด์ความเข้มข้น 0.5 โมลาร์ และกรดไฮโดรคลอริก 0.5 โมลาร์ ค่า%ประสิทธิภาพในการละลายของคาร์บอนไดออกไซด์ (ปริมาณคาร์บอนไดออกไซด์ที่ละลายน้ำ (กรัม) / ปริมาณคาร์บอนไดออกไซด์ที่ป้อนเข้าไป (กรัม)) ได้ถูกคำนวณขึ้น จากการทดลองพบว่า การเพิ่มค่าพีเอชสามารถทำให้เกิดการละลายของคาร์บอนไดออกไซด์ในน้ำได้มากขึ้นและมีประสิทธิภาพมากขึ้น การเพิ่มพื้นที่สัมผัสระหว่างแก๊สและของเหลวและการกักแก๊สในน้ำทำให้การละลายของคาร์บอนไดออกไซด์ดีขึ้นเล็กน้อย การเพิ่มความสูงสามเท่าของหอป้อนอากาศเท่ากับ 1 เมตรเป็น 3 เมตรให้%ประสิทธิภาพโดยรวมดีขึ้นแต่ไม่เป็นสัดส่วนโดยตรงกับความสูง นอกเหนือจากนี้ ปริมาณของคาร์บอนไดออกไซด์ในรูปแก๊สมีค่าลดลงตามระดับความสูงทำให้มีปริมาณของคาร์บอนไดออกไซด์ลดลงที่ระดับความสูงที่เพิ่มขึ้น ที่อัตราการไหลของคาร์บอนไดออกไซด์ที่สูงขึ้น ก๊าซคาร์บอนไดออกไซด์มีระยะเวลาในการสัมผัสกับสารละลายไม่เพียงพอและถูกปล่อยสู่บรรยากาศอย่างไม่ได้ใช้ประโยชน์ส่งผลให้เกิด%ประสิทธิภาพต่ำ ระบบ "Circulating Counterflow Contactor -C.C.C." ได้ถูกออกแบบให้มีการไหลของแก๊สและของเหลวไหลสวนทางกันเพื่อเพิ่มระยะเวลาในการสัมผัสและการผสมที่ดีขึ้น C.C.C. ให้%ประสิทธิภาพที่สูงอย่างคงที่ในช่วง 34-56% ในกรณีอัตราการไหลวนที่เหมาะสมที่สุดที่ 2 ลิตรต่อนาที ที่ระดับความเค็มของน้ำทะเลมากขึ้นพบว่า การละลายของคาร์บอนอินทรีย์โดยรวมลดลง นอกเหนือจากนี้ผลของไบคาร์บอเนตที่ผลต่อการเจริญเติบโตของจุลสาหร่ายได้ถูกศึกษาโดยปรับค่าพีเอชเริ่มต้นในช่วง 6-9 โซเดียมไบคาร์บอเนตที่ความเข้มข้น 30 พีพีเอ็มได้ถูกป้อนเข้าสู่ระบบการเลี้ยงโดยค่าพีเอชที่ 6 และ 7 แสดงให้เห็นถึงค่าพีเอชเริ่มต้นที่เหมาะสมที่สุดในการเลี้ยงโดยความเข้มข้นของเซลล์ที่มากที่สุดและอัตราการเจริญเติบโตจำเพาะแตกต่างกันเล็กน้อย การเพิ่มความเข้มข้นของโซเดียมไบคาร์บอเนตจาก 30 พีพีเอ็มเป็น 80 และ 200 พีพีเอ็มไม่ได้ส่งผลต่อการเจริญเติบโตอย่างเห็นได้ชัด น้ำจากการละลายของคาร์บอนไดออกไซด์จากระบบ C.C.C. ได้ถูกป้อนเข้าสู่ระบบการเลี้ยงจุลสาหร่าย *C. vulgaris* และผลแสดงให้เห็นชัดเจนว่าความเข้มข้นเซลล์ที่สูงที่สุดและอัตราการเจริญเติบโตจำเพาะมากกว่าการใช้โซเดียมไบคาร์บอเนตที่ละลายน้ำ

ภาควิชา วิศวกรรมเคมี
สาขาวิชา วิศวกรรมเคมี
ปีการศึกษา.....2553

ลายมือชื่อนิสิต
ลายมือชื่อ อ.ที่ปรึกษาวิทยานิพนธ์หลัก.....

5270459521: MAJOR CHEMICAL ENGINEERING

KEYWORDS: CARBON DIOXIDE / CO₂ / GAS DISSOLUTION / CAPTURE AND STORAGE / INORGANIC CARBON / BICARBONATE / CARBONATE / MICROALGAL CULTIVATION / CHLORELLA VULGARIS

YOSSARAN PICHIANSOONTORN: ACCELERATING MICROALGAL GROWTH WITH CO₂ TRANSFORMATION. THESIS ADVISOR: ASSOC. PROF. PRASERT PAVASANT, Ph.D., 99 pp.

The maximising carbon dioxide capture in the water as inorganic carbon source for accelerating microalgal growth was carried out where the effects of pH, gas-liquid contacting area, height, gas flowrate and salinity on dissolved Total Inorganic Carbon (TIC) concentration were observed. The experiments were conducted in 1-3 m high bubble column and packed column. The pH of the demineralised water was adjusted as required using NaOH 0.5 M and HCl 0.5 M. %Efficiency of CO₂ dissolution (Dissolved CO₂ (g)/ Input CO₂ (g)) was then computed. From the findings, an increase in pH could lead to a greater dissolution of CO₂ resulting in a greater effluent TIC concentration and high %CO₂ dissolution efficiency. Adding gas-liquid contact area and gas hold up (ϵ_g) caused a slightly greater dissolution of CO₂. A triple increase in height from 1 m to 3 m in packed column gave the better overall %efficiency but not in a direct proportional to the height. Furthermore, the gas phase CO₂ decreased along the axial position resulting in a lesser quantity of CO₂ at higher position in the column. At high CO₂ flowrate, CO₂ did not have enough contact time with the solution and wastefully released to the atmosphere causing low %efficiency. The design of the –“Circulating Counterflow Contactor –C.C.C.” system was employed where the liquid and gas were counter-flowed to enhance the contact time and better mixing. The C.C.C. offered the steadily high %efficiency not only in early stage but also later stage in the range of 34-56% at the liquid flowrate of 2 LPM was employed. Higher degree of salinity was found to lower the dissolution of TIC in the solution. Additionally, the effect of bicarbonate on microalgal growth was examined by initially manipulating pH in range 6-9. NaHCO₃ at 30 ppm was fed into the cultivation system where pH 6 and 7 exhibited most suitable initial pH the in which maximum cell concentration and specific growth rate were slightly different. An increase in NaHCO₃ concentration from 30 to 80 and 200 ppm did not seem to have significant effect on the growth. CO₂ dissolution from C.C.C. system was also employed to cultivate *C. vulgaris* and obviously the results illustrated a higher growth where the maximum cell concentration and specific growth rate were higher than using dissolved NaHCO₃.

Department: Chemical Engineering..

Academic Year:2010.....

Student's Signature.....

Advisor's Signature.....

ACKNOWLEDGEMENTS

I am deeply indebted to my thesis advisor, Associate Professor Dr. Prasert Pavasant, Department of Chemical Engineering, Chulalongkorn University. This thesis would not be accomplished without him and his excellent supervision. He always motivates me to actualize the goal I have set. I would like to say that thank you very much for everything given to support me and also a lot of chances provided to me. I wish I might study a Ph.D. with him after I fulfilled my dream as a field engineer and I would like to be an active researcher like him.

I would like to express my gratitude to my thesis chairman, Associate Professor Dr. Tharathon Mongkhonsi, thesis committee, Dr. Jirdsak Tscheikuna, Department of Chemical Engineering, Chulalongkorn University and external examiner Associate Professor Dr. Tawan Sooknoi, Department of Chemistry, King Mongkut's Institute of Technology Ladkrabang for their worthy time on my thesis.

I would like to deeply thank Supersert's team (P'Tik for a lot of motivation and advice, P' Big for great support and reactor set-up, P' Max for his skillful techniques, P' Toey for her great tutorial in microalgal cultivation, P' Term for electrical devices, P' Note for inspiration, P' Mod Chattip for her support, P'Mod Mode, P' Aim, P' Dump and P' Aom for their useful advices. I'm grateful for your supports.

This work cannot be succeeded if it was without research grants from PTT and "Chula Cluster". I am deeply appreciated for very baht that I spent on my research.

I would like to sincerely thank the National Nanotechnology Center (NANOTEC) for permission of using TOC Analyser for Total Inorganic Carbon concentrations analyse. I would like to especially thank P' Porn for instrument training and her support. NANOTEC members: P' Toey, P' Beer, P' Job, and etc., I'm appreciated with your warm welcome.

I am appreciated of my friends' support: my OSK 123 friends (Keaw, Guard, F, Oak and Tu), my ChemTech friends (Elf, Fye, Tie, Ake, Poy, Pahn, Phai, Pla and Ed) and my ChemEn friends (Nhu, Bo, Preaw and Best).

I could not accomplish without the loves from my family. I would like to express my deep sense of appreciation to my parent and sister for their strong supports, encouragements and inspiration. Finally, I would like to thank Jane. You always stand by my side and give me wonderful times.

ศูนย์วิจัยทรัพยากร
จุฬาลงกรณ์มหาวิทยาลัย

CONTENTS

	Page
ABSTRACT IN THAI	iv
ABSTRACT IN ENGLISH	v
ACKNOWLEDGEMENTS	vi
CONTENTS	vii
LIST OF TABLES	xi
LIST OF FIGURES	xii
CHAPTER I Introduction	1
1.1 Motivation.....	1
1.2 Objectives.....	2
1.3 Scopes of research.....	2
CHAPTER II Theoretical Background and Literature Review	3
2.1 Global warming and CO ₂ as greenhouse gas.....	3
2.1.1 Global warming and greenhouse gases.....	3
2.2.2 CO ₂ as greenhouse gas.....	3
2.2 CO ₂ removal methods.....	4
2.2.1 CO ₂ removal via absorption processes.....	4
2.2.2 CO ₂ removal via carbonation processes.....	6
2.2.3 CO ₂ removal via adsorption processes.....	8
2.2.4 CO ₂ removal via membrane contactors.....	9
2.2.5 CO ₂ removal via algal cultivation.....	11
2.3 CO ₂ Removal via algal cultivation (CO ₂ Bio-mitigation).....	12
2.4 CO ₂ and bicarbonate as inorganic carbon source for microalgal uptake...	15
2.5 CO ₂ solubility in the water.....	17

	Page
2.6 Literature Review.....	21
CHAPTER III Materials and Methods.....	26
3.1 Experimental setup.....	27
3.1.1 Combined effect of system design for CO ₂ dissolution.....	27
3.1.2 Effect of bicarbonate as inorganic carbon source for fresh water microalgae.....	30
3.2 Experimental Procedure.....	30
3.2.1 Maximising CO ₂ dissolution in bubble column.....	30
3.2.1.1 Study of pH effect.....	32
3.2.1.2 Study of salinity effect.....	32
3.2.1.3 Study of gas-liquid contact area.....	33
3.2.1.4 Study of optimal gas flowrate effect.....	33
3.2.1.5 Study of height and gas-liquid contact area effect.....	34
3.2.1.6 Study of combined effect of optimal conditions.....	34
3.2.2 Effect of bicarbonate on microalgal growth.....	35
3.2.2.1 Cultivation of Chlorella vulgaris without NaHCO ₃ added and pH adjustment.....	36
3.2.2.2 Effect of bicarbonate and pH on microalgal growth.....	36
3.2.2.3 Effect of 200 ppm of NaHCO ₃ on microalgal growth.....	37
3.2.2.4 Effect of CO ₂ dissolution water from optimal combined effect bubble column.....	37
3.3 Analyses.....	38
3.3.1 Determination of Total Inorganic Carbon.....	38
3.3.2 Determination of %CO ₂ dissolution efficiency.....	39
3.3.3 Determination of cell concentration.....	40
3.3.4 Determination of specific growth rate.....	41

	Page
CHAPTER IV Results and Discussion	42
4.1 Maximising CO ₂ dissolution in bubble column.....	42
4.1.1 Effect of pH on total inorganic carbon dissolved in the water.....	42
4.1.2 Effect of gas-liquid contacting area on total inorganic carbon dissolved in the water.....	45
4.1.3 Effect of gas-liquid contacting area on total inorganic carbon at pH 10 in 3 m high packed column.....	51
4.1.4 Effect of gas flowrate on CO ₂ dissolution from 10-40 cc/min fed into the 1 and 2m high bubble column.....	53
4.1.5 Effect of salinity on CO ₂ dissolution.....	59
4.1.6 CO ₂ dissolution using Circulating Counterflow Contactor (C.C.C.).....	61
4.2 Accelerating microalgal growth with bicarbonate as inorganic carbon source.....	63
4.2.1 Cultivation of <i>C. vulgaris</i> with NaHCO ₃ at various pH range.....	63
4.2.2 Cultivation of <i>C. vulgaris</i> with high concentration of NaHCO ₃ and CO ₂ dissolved water from C.C.C. as inorganic carbon at pH 7.....	65
CHAPTER V Conclusion	68
5.1 Conclusions.....	68
5.2 Contributions.....	69
5.3 Recommendations / Future works.....	70
REFERENCES	71
APPENDICES	78
APPENDIX A : TOTAL INORGANIC CARBON ANALYSE EXPERIMENTAL DATA.....	79

	Page
APPENDIX B : CULTIVATION OF C. VULGARIS WITH BICARBONATE EXPERIMENTAL DATA.....	90
APPENDIX C : SAMPLE CALCULATIONS.....	95
APPENDIX D : PUBLICATIONS.....	98
BIOGRAPHY	99



ศูนย์วิทยทรัพยากร
จุฬาลงกรณ์มหาวิทยาลัย

LIST OF TABLES

		Page
Table 2.6.1	Summary of CO ₂ removal rate via amine processes.....	22
Table 2.6.2	Summary of CO ₂ removal rate via algal cultivation.....	25
Table 4.1.1	%Efficiency of CO ₂ dissolution at various pH levels.....	45
Table 4.1.2	%Efficiency of CO ₂ dissolution in packed column at various pH levels and positions.....	50
Table 4.1.3	%Efficiency of CO ₂ dissolution in packed column at pH 10 and every 1 meter position.....	53
Table 4.1.4.1	%Efficiency of CO ₂ dissolution in 1 m high column.....	55
Table 4.1.4.2(a)	%Efficiency of CO ₂ dissolution in 2 m high column: samples collected at 1 m position.....	58
Table 4.1.4.2(b)	%Efficiency of CO ₂ dissolution in 2 m high column: samples collected at 2 m position.....	58
Table 4.1.5	%Efficiency of CO ₂ dissolution at various salinity levels from 0-30 ppt.....	60
Table 4.1.6	%Efficiency of CO ₂ dissolution using recycle flow of 1-3 LPM.....	62
Table 4.2.1	Maximum cell concentration and specific growth rate (μ) of <i>Chlrollera vulgaris</i> cultivation with 30 ppm NaHCO ₃ as inorganic carbon source at various initial pH conditions.....	64
Table 4.2.2	Maximum cell concentration and specific growth rate (μ) of <i>Chlrollera vulgaris</i> cultivation with various amount of NaHCO ₃ as inorganic carbon source at initial pH 7 condition.....	67

LIST OF FIGURES

		Page
Figure 2.1	Process flow diagram for CO ₂ recovery from the flue gas by chemical absorption	6
Figure 2.2	Process flow diagram for CO ₂ recovery from the flue gas by Benfield process or carbonation process.....	8
Figure 2.3.1	<i>Chlorella sp.</i> open system cultivation ponds.....	13
Figure 2.3.2	<i>Physcomitrella patens</i> photobioreactor for biopharmaceutical.....	14
Figure 2.5.1	The relationship between solubility of CO ₂ in the water (in g·10 ⁻² ml ⁻¹) at various temperature (°C) at 1 atm pressure	19
Figure 2.5.2	The various fraction of carbonate species in pH range from 4 to 13.....	20
Figure 3.1	Experimental diagram: Maximising CO ₂ dissolution in bubble column....	26
Figure 3.2	Experimental diagram: Study of bicarbonate as inorganic carbon source for fresh water microalgae cultivation.....	27
Figure 3.3	Experimental setup for CO ₂ fed bubble column.....	28
Figure 3.4	One cm diameter packing material.....	29
Figure 3.5	Experimental setup for Circulating Counterflow Contactor.....	30
Figure 3.6	Experimental setup for cultivation of <i>Chlorella vulgaris</i> in sharing light source bubble columns.....	31
Figure 4.1.1	Total Inorganic Carbon time profile at various pH levels.....	44
Figure 4.1.2.1	Total Inorganic Carbon time profile at various pH levels in bubble column with packing material (a) at top of the column (b) at middle of the column.....	49
Figure 4.1.2.2	Total Inorganic Carbon time profile at pH 10 level in different column....	50
Figure 4.1.3	Total Inorganic Carbon time profile: samples collected various axial positions in the 3 meter high bubble column.....	52
Figure 4.1.4.1	Total Inorganic Carbon at different time in 1 m bubble column: Effect of gas flowrate from 10-40 cc·min ⁻¹	54

Figure 4.1.4.2	Total Inorganic Carbon at different time: effect of gas flowrate from 10-40 cc·min ⁻¹ on Total Inorganic Carbon concentration and samples collected (a) at 1m height (b) at 2m height.....	57
Figure 4.1.5	Total Inorganic Carbon time profile and salinity levels from 0-30 ppt.....	60
Figure 4.1.6	Total Inorganic Carbon at different time at various recirculating flows in the gas-liquid contacting bubble column, using recycle flow in a range of 1-3 LPM (Litres per minute).....	62
Figure 4.2.1	Growth curve of <i>Chlorella vulgaris</i> cultivation with 30 ppm NaHCO ₃ as inorganic carbon at various pH ranges from 6-9.....	64
Figure 4.2.2	Growth curve of <i>C. vulgaris</i> cultivated with various 0, 30, 80 and 200 ppm NaHCO ₃ and water from CO ₂ dissolved water from C.C.C. as inorganic carbon at initial pH 7 condition.....	66

CHAPTER I

INTRODUCTION

1.1 Motivations

At present, the global warming caused by emissions of anthropogenic greenhouse gases is one of the most serious environmental problems. Carbon dioxide (CO₂) is the main component of greenhouse gases and an increase in CO₂ at atmospheric level is accelerating global climate change. Global average temperature has increased by 0.6°C per year since 1900, by the end of the twenty-first century; temperature may increase drastically at around 1.4–5.8°C in total (Pipitone and Bolland, 2009). Effects of global warming vary in nature, but they will surely have their global consequences such as changes in weather, sea level rise, etc.

To mitigate climate change, reductions in CO₂ emissions are required. There are many CO₂ reduction approaches including physical, chemical, and biological methods, for example; adsorption by hydrogel membrane and wetted porous material (physical methods) (Ishibashi et al., 1999 and Yokoyama, 2003), absorption by amine process (Je et al., 2009; You et al., 2008; Bai et al., 2005), cyclic carbonation/de-carbonation reactions process (chemical methods) (Abanades et al., 2004b; Wang et al., 2004) and CO₂ biological uptake via photosynthetic living organisms (biological method) (Sydney et al., 2010; Ryu et al., 2008; Huntley et al., 2007), etc. The world's most widely used method is amine process using gas scrubber or absorber to sweetening natural gas and carbonation process for ammonia plant. Among these approaches, the biological method using microalgal photosynthesis is recently considered as an effective method to remove CO₂ from stack or flue gas. By this approach, CO₂ is turned into the form of microalgal biomass by photosynthesis. Most microalgae use CO₂ as an inorganic source for their growth through photosynthetic pathway, and CO₂ naturally is transformed to oxygen, biomass and many useful chemical substances such as lipids and proteins. Due to mass transfer limitation between gas bubble and liquid, CO₂ in gaseous form cannot dissolve well as aqueous solution at

a desired rate, and in most cases, CO₂ is freely released to the atmosphere. Other CO₂ transformation is required in an alternative choice which helps sequester CO₂ from stack gas.

This study aims to investigate the capture and storage of CO₂ into other inorganic soluble forms such as aqueous CO₂, carbonate and bicarbonate compounds which can potentially be consumed by microalgae, and also to examine the possibility in using this dissolved CO₂, most likely in bicarbonate form, in cultivating microalgae.

1.2 Objectives

The main objective of this work was twofold. Firstly, the work attempted to sequester CO₂ by maximizing its dissolution in the special design gas-liquid contactor. Secondly, the use of dissolved carbon dioxide in the form of bicarbonate CO₂ in the cultivation of microalgae, *Chlorella vulgaris*, at various pH ranges was examined.

1.3 Scopes of the research

1.3.1 The determination of optimal conditions for the CO₂ dissolution in bubble columns was performed by varying the following parameters:

- pH level at 6, 8 and 10
- Height of reactor from 1 to 3 meters
- Salinity in a range of 0-30 ppt (parts per thousand)
- Gas flow pathway induced by packing material
- Liquid flow configuration induced by recirculating liquid in the gas-liquid contacting bubble column, using recycle flow in a range of 1-3 LPM (Liters per minute)

1.3.2 The effect of bicarbonate on microalgal growth was examined by initially manipulating pH in range 5-9, and varying initial bicarbonate concentration in the range of 0-200 mg·L⁻¹. Furthermore, the algal growth under the addition of CO₂ captured from Section 1.3.1 was also investigated where the efficiency of the cultivation systems was indicated by Cell concentration and Specific growth rate.

Chapter II

Theoretical Backgrounds and Literature Review

2.1 Global warming and CO₂

2.1.1 Global warming and greenhouse gases

Global warming is an increase in average temperature of the world's atmosphere and oceans. Global warming has generally been known to be a consequence of an increase in concentrations of greenhouse gases resulting from human's activities e.g. fossil fuel combustion, deforestation and electricity generation from power plant. Global average temperature has increased by 0.6°C per year since 1900, and by the end of the twenty-first century, temperature may increase by a drastic figure of around 1.4–5.8°C in total (Pipitone and Bolland, 2009) resulting in the change of weather system, melting ice and also sea level rise. The greenhouse gases like nitrous oxide, methane and especially carbon dioxide are playing crucial role in the world's global warming phenomenon at the present time. The excessive emission of these gases is the major cause of global warming as these gases trap heat in the earth's atmosphere. To decrease the effect of global warming, greenhouse gases must be controlled or diminished from emitting sources. Global warming mitigation is becoming increasingly important as the effects of climate change are becoming apparent all around the world.

2.1.2 CO₂ as greenhouse gas

CO₂ gas is playing a major role in global warming. When CO₂ is released to the atmosphere, it acts like blanket over the planet by trapping long-wave radiation from leaving the Earth's surface and raising the average temperature. The growth rate of atmospheric carbon dioxide (CO₂), the largest human contributor to human-induced climate change, is increasing rapidly. Recent growth of the world economy combined with an increase in its carbon intensity has led to rapid growth in fossil fuel CO₂ emissions. CO₂ is the largest contributor to this effect as it is a long-lived gas and its emission increases each year. From these reasons, international

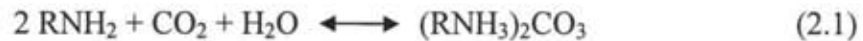
courtesy rules for CO₂ reduction was proposed e.g. Kyoto protocol and EU's carbon credit regulations

2.2 CO₂ removal methods

2.2.1 CO₂ removal via absorption processes

There are several commercial available process technologies which can in principle be used for CO₂ capture from flue gases. However, comparative assessment studies have shown that absorption processes based on chemical solvents are currently the preferred option for post-combustion CO₂ capture (Je et al., 2009; You et al., 2008). At present, absorption processes offer high capture efficiency and selectivity, and lowest energy consumption and costs when compared with other existing post-combustion CO₂ capture system. Absorption processes in post-combustion capture make use of the reversible nature of the chemical reaction of an aqueous alkaline solvent, usually an amine, with an acid or sour gas. The process flow diagram is presented in Figure 2.1. After cooling the flue gas, it is brought into contact with the solvent in an absorber. A blower is required to overcome the pressure through the absorber. At absorber temperatures between 40 and 60°C, CO₂ is bound by chemical solvent in the absorber. The flue gas then undergoes a water wash section to balance water in the system and to remove any solvent droplets or solvent vapor carried over, and then it leaves the absorber. It is possible to reduce CO₂ concentration in the exit gas down to very low values, as a result of the chemical reaction in the solvent but lower exit concentrations tend to increase the height of the absorption vessel. The rich solvent which contains the chemically bound CO₂ is then pumped to the top of stripper (or regeneration of chemical solvent in the stripper at elevated temperatures (100-140 °C) at pressure not very much higher than atmospheric pressure. Heat is supplied to the reboiler to maintain the regeneration conditions. This leads to a thermal energy penalty as a result of heating up the solvent, providing the required desorption heat for removing the chemically bound CO₂ and for steam production which acts as a stripping gas. Steam is recovered in the condenser and fed back to stripper, whereas the CO₂ product leaves the stripper. The lean solvent, containing far less CO₂ is then pumped back to the absorber via the lean-rich heat exchanger and a cooler to bring it down to the absorber temperature level.

Reactions are described below:



R = C₂H₄OH group

The key parameters determining the technical and economic operation of a CO₂ absorption system are

- Flue gas flow rate –The flue gas flow rate will determine the size of the absorber.
- CO₂ content in flue gas –Since flue gas is usually at atmospheric pressure, the partial pressure of CO₂ will be at 3-15 kPa. Under these low CO₂ partial pressure conditions, aqueous amines (chemical solvents) are the most suitable absorption solvents (Kohl and Nielsen, 1997).
- CO₂ removal –In practice, the exact recovery choice will lead to a taller absorption column, higher energy penalties, and hence, increasing cost.
- Solvent flow rate –The solvent flow rate will determine the size of most equipment apart from the absorber. For a given solvent, the flow rate will be fixed by the previous parameters described above and also the chosen CO₂ concentrations within the lean and rich solutions.

ศูนย์วิทยทรัพยากร
จุฬาลงกรณ์มหาวิทยาลัย

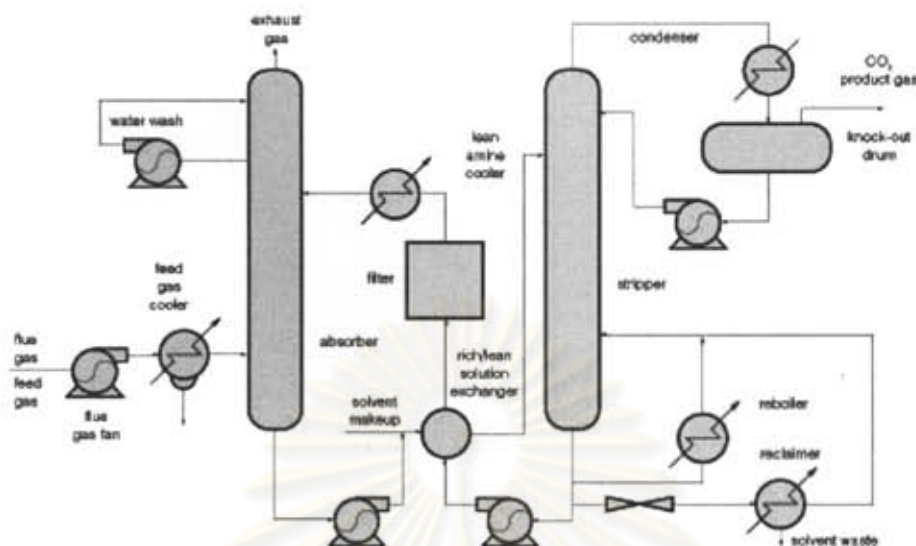


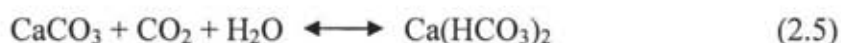
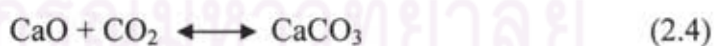
Figure 2.1 Process flow diagram for CO₂ recovery from the flue gas by chemical absorption (Metz et al., 2005)

2.2.2 CO₂ removal via carbonation processes

There are post-combustion systems being proposed that make use of regenerable solid sorbents to remove CO₂ at relatively high temperatures. The use of high temperatures in the CO₂ separation step has the potential to reduce efficiency penalties with respect to wet-absorption methods. In principle, they all follow the scheme shown in Figure 2.2, where the combustion flue gas is put in contact with the sorbent in a suitable reactor to allow the gas-solid reaction of CO₂ with the sorbent (usually the carbonation of metal oxide). The solid can be easily separated from gas stream and sent for regeneration in a different reactor. One key component for the development of these systems is obviously the sorbent itself with good CO₂ absorption capacity and chemical and mechanical stability for long period of operation in repeated cycle. Solid sorbents investigated for large-scale CO₂ capture purposes are sodium and potassium dioxides and carbonates (to produce bicarbonate). They are usually supported on a solid substrate (Hoffman et al., 2002; Green et al., 2002). Also, high temperature Li-based and CaO-based sorbents are suitable candidates. The use of lithium-containing compounds (lithium, lithium-zirconia and lithium-silica oxides) in a carbonation-calcination cycle, was first investigated in Japan (Nakagawa and Ohashi, 1998). They reported that the performance of these sorbents was

very good, with very high reactivity in wide range of temperatures below 700°C, rapid regeneration at higher temperatures and durability in repeated capture-regeneration cycles. The use of CaO as a regenerable CO₂ sorbent has been proposed in several processes in the 19th century. The carbonation reaction of CaO to separate CO₂ from hot gases (T > 600 °C) is very fast and the regeneration of the sorbent by calcining the CaCO₃ into CaO and pure CO₂ is favoured at T > 900 °C (at a partial pressure of CO₂ of 0.1 MPa). The basic separation principle using this carbonation-calcination cycle for post-combustion system was first proposed by Shimizu et al. (1999). The effective capture of CO₂ by CaO has been demonstrated in a small pilot fluidized bed (Abanades et al., 2004a). Other combustion cycles incorporating capture of CO₂ with CaO that might not need O₂ are being developed, including one that works at high pressures with simultaneous capture of CO₂ and SO₂ (Wang et al., 2004). One weak point in all these processes is that natural sorbents (limestones and dolomites) deactivate rapidly, and a large make-up flow of sorbent (of the order of the mass flow of fuel entering the plant) is required to maintain the activity in the capture-regeneration loop (Abanades et al., 2004b). Although the deactivated sorbent may find application in the cement industry and the sorbent cost is low, many ranges of method to enhance the activity of Ca-based CO₂ sorbents are being pursued by several research around the world. To improve CO₂ absorption mass transfer and to inhibit corrosion, proprietary activators and inhibitors are added. These systems known as "activated hot potassium carbonate" (AHPC) systems including the original Benfield activator, DEA (Diethanolamine) show that the full capacity of the "hot pot" family of processes requires a feed CO₂ partial pressure of about 700 kPa.

Reactions are described below:



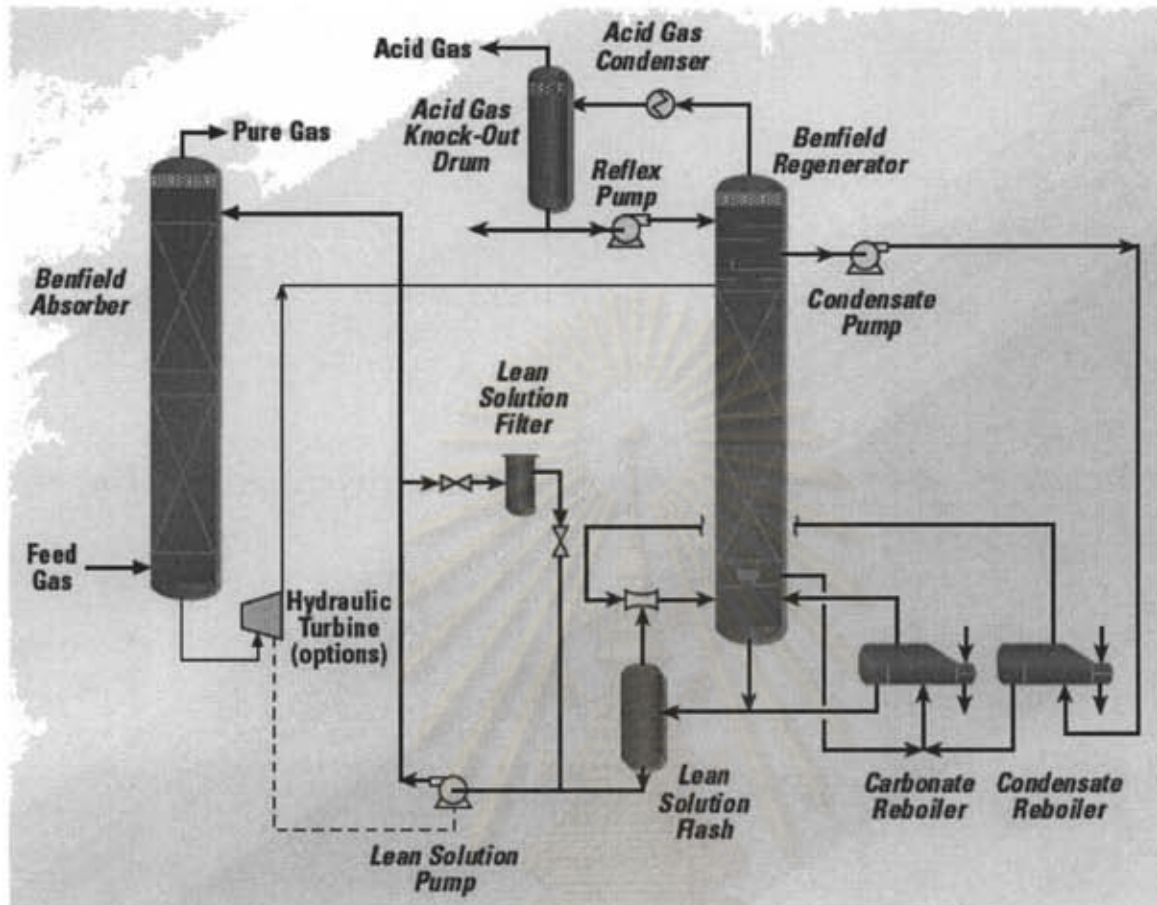


Figure 2.2 Process flow diagram for CO₂ recovery from the flue gas by Benfield process or carbonation process (UOP LLC, 2000)

2.2.3 CO₂ removal via adsorption processes

In the adsorption process for flue gas CO₂ recovery, molecular sieves or activated carbons are used in adsorbing CO₂. Desorbing CO₂ is then by the pressure swing operation (PSA) or temperature swing operation (TSA). Most applicants are associated with pressure swing adsorption (Ishibashi et al., 1999 and Yokoyama, 2003). Much less attention has been focused on CO₂ removal via temperature swing adsorption due to the longer cycle times needed to heat up the bed of solid particles during sorbent regeneration. For bulk separations at large scale, it is also essential to limit the length of the unused bed and therefore opt for faster cycle times.

Adsorption processes have been employed for CO₂ removal from synthesis gas for hydrogen production. It has not yet reached a commercial stage for CO₂ recovery from flue gases. It can be concluded based on mathematical models and pilot-scale data that industrial adsorption process might be feasible. A serious drawback of all adsorptive methods is the necessity to treat the gaseous feed before CO₂ separation in an adsorber. In many cases gases have to be also cooled and dried, which limits the attractiveness of PSA, TSA or ESA (electric swing adsorption) compared with capture by chemical absorption described in previous sections. The development of a new generation of materials that would efficiently adsorb CO₂ will undoubtedly enhance the competitiveness of adsorptive separation in a flue gas application.

2.2.4 CO₂ removal methods via membrane contactors

Membrane processes are used commercially for CO₂ removal from natural gas at high pressure and at high CO₂ concentration. In flue gases, the low CO₂ partial pressure difference provides a low driving force for gas separation. The removal of carbon dioxide using gas separation with polymeric membranes results in not only energy penalties compared with a standard chemical absorption process, but also the maximum percentage of CO₂ removed which is lower than for a standard chemical absorption processes (Herzog et al., 1991, Van der Sluijs et al., 1992 and Feron, 1994).

The membrane option currently receiving the most attention is a hybrid membrane-absorbent (or solvent) system. These systems are being developed for flue gas CO₂ recovery. Hybrid membrane systems enhance membrane to provide a very high surface to volume ratio for mass exchange between gas stream and solvent resulting in a very compact system. This results in membrane contactor system in which the membrane forms a gas permeable barrier between a liquid and a gaseous phase. In cases of non-porous membranes, CO₂ dissolves in the membrane and diffuse through the pores and are absorbed by the liquid. The contact surface area between gas and liquid phases is maintained by the membrane and is independent of the gas and liquid flow rate. The selectivity of the partition is primarily determined by the absorbent (solvent). Absorption in the liquid phase is determined either by physical partition or by a chemical reaction.

The advantage of membrane/solvent systems are avoid of operation problems where gas and liquid flows are in direct contact. Operation problems avoided include foaming, flooding and channeling. Furthermore, the use of compact membranes result in a smaller equipment sizes with capital cost reductions. The alternative of a suitable combination of solvent and membrane material is very important. The material characteristics should be avoided at operating pressure gradients of typically 50-100 KPa while the transfer of gas is not hindered. Membrane/solvent systems can be both used in the absorption as well as in desorption step.

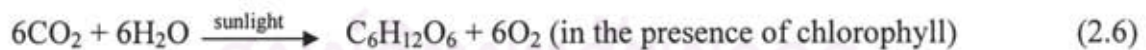
Research and development efforts have also been reported in the area of facilitated transport membranes. An important class of facilitated transport membranes is the so-called liquid membrane in which carrier is dissolved into a liquid contained in a membrane. For CO₂ separation, carbonates, amines and molten salt hydrates have been suggested as carriers (Feron, 1992). Porous membranes and ion-exchange membranes have been employed as the support. Until now, supported liquid membranes have been only study in a laboratory scale. Practical problems associated with supported liquid membranes are membrane stability and liquid volatility. Recent development work has focused on the following technological options that are applicable to both CO₂/N₂ (i.e. Amine process) and CO₂/H₂ (i.e. Fuel cell and Syngas purification) separations, examples include:

- Amine-containing membranes (Teramoto et al., 1996),
- Membranes containing potassium carbonate polymer gel membrane (Okabe et al., 2003),
- Membranes containing potassium carbonate-glycol (Chen et al., 1999),
- Dendrimer-containing membranes (Kovvali and Sirkar, 2001),
- Poly-electrolyte membranes (Quin and Laciak, 1997).

2.2.5 CO₂ removal via algal cultivation

The biological method using microalgal photosynthesis is recently considered as an effective method to remove CO₂ from stack or flue gas. By this approach, CO₂ is turned into the form of microalgal biomass by photosynthesis. Carbon fixation refers to process through which gaseous carbon dioxide is converted into a solid compound. It mostly refers to the processes found in autotrophs (organisms that produce their own food), usually driven by photosynthesis. Most microalgae use CO₂ as an inorganic source for their growth through photosynthetic pathway, and CO₂ naturally is transformed to oxygen, biomass and many useful chemical substances such as lipids and proteins. Microalgae can fix carbon dioxide from different sources, such as CO₂ from the atmosphere and from industrial exhaust gases (e.g. flue gas and flaring gas), and fixed CO₂ in the form of soluble carbonates (e.g., NaHCO₃ and Na₂CO₃). Photosynthetic organisms are called photoautotroph, since they can create their own food. In plants, algae and cyanobacteria, photosynthesis uses carbon dioxide and water and converts to sugar (glucose), releasing oxygen as a waste product. Glucose may be used directly by the plant for its own metabolic needs during cellular respiration. Excess glucose also can be converted into other molecules (fiber, starch, protein and fat) for structural or energy-storage purposes.

Photosynthetic reaction is described below:



More informative CO₂ removal via algal cultivation is described in Section 2.3.

2.3 CO₂ Removal via algal cultivation (CO₂ Bio-mitigation)

Biological CO₂ mitigation has attracted much attention as an alternative strategy because it leads to production of biomass energy in the process of CO₂ fixation through photosynthesis (Ryu et al., 2008; de Moraes and Costa et al., 2007). Biological CO₂ mitigation can be carried out by plants and photosynthetic microorganisms (photosynthesis reaction is described in Section 2.2.5). However, the potential for increased CO₂ capture in agriculture by plants has been estimated to contribute only 3–6% of fossil fuel emissions (Skjanes et al., 2007), largely due to the slow growth rates of conventional terrestrial plants

Microalgae, a group of fast-growing unicellular or simple multicellular microorganisms, have the ability to fix CO₂ while capturing solar energy with an efficiency of 10 to 50 times greater than that of terrestrial plants (Li et al., 2008). The microalgae-for-CO₂-mitigation or CO₂ fixation via microalgae cultivation provides numerous advantages.

Firstly, microalgae have much higher growth rates and CO₂ fixation abilities compared to conventional forestry, agricultural, and aquatic plants (Li et al., 2008). Secondly, it could completely recycle captured CO₂ because carbon dioxide is converted into the chemical substances via photosynthesis. In comparison, the chemical reaction-based CO₂ removal approaches as previous discussed above, have disposal problems because both the captured CO₂ and the wasted absorbents need to be disposed (Bonenfant et al., 2003). Thirdly, as mentioned in the previous section, chemical reaction-based CO₂ mitigation approaches are energy-consuming and costly processes (Lin et al., 2003; Resnik et al., 2004). On the other hand, CO₂ bio-mitigation using microalgae could be made profitable from the production of biofuels and other useful bioproducts. Finally, the microalgal CO₂ bio-mitigation could be made more economically cost-effective and environmentally sustainable, especially when it is combined with other processes such as wastewater treatment integrated with other facilities.

A number of microalgal species have been shown to be able to utilize carbonates such as Na₂CO₃ and NaHCO₃ as inorganic sources for cell growth (Huertas et al., 2000a). They fix CO₂ by chemical reaction to produce bicarbonates and carbonates and use as the latter carbon source for microalgal cultivation. These bicarbonates and carbonates uptake pathway by active transport in microalgae are mainly described in Section 2.4.

There are two main methods in which algae can be cultivated. One of the methods is to cultivate algae in an open pond or lake. This type of system is considerably cheap and allows for large production capacities. However, because this is an open system, the algae are exposed to natural, uncontrolled conditions such as water temperature and lighting conditions. There is also a risk of contamination by other organisms. This often causes problems with the open pond cultivating systems. A cover or greenhouse may be used to cover the pond to increase production by eliminating some of the disturbances associated with open systems.

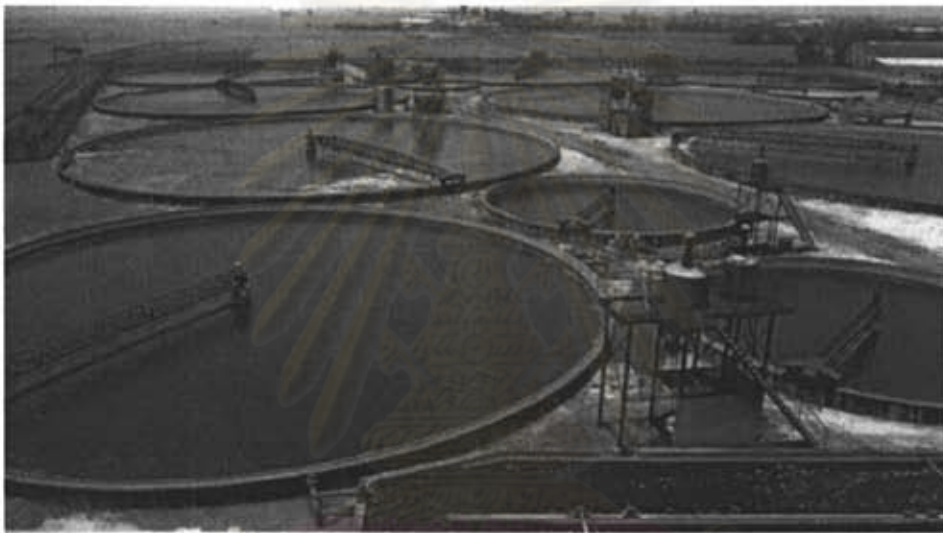


Figure 2.3.1 *Chlorella sp.* open system cultivation ponds (Continex, 2009)

Another method in which microalgae can be cultivated is by using a photobioreactor. A photobioreactor contains a light source and is a closed system. The photobioreactor can be set up like a batch reactor or a continuously harvesting reactor. As a microalgal photobioreactor is a totally enclosed system it is generally more expensive than an open system. However, there are several major advantages as the bioreactor can prevent or at least minimize contamination and allows easier cultivation of one algae strain. It also offers better control over a range of other growing conditions, like pH, light, carbon dioxide, and temperature. To enhance productivity of microalgae with CO₂, flue gases from emitting sources can be directed through the integrated microalgal reactor. CO₂ is taken up by the microalgae, directly recycled in the form of biomass

and derived products. Several algal cultivation systems are equipped with CO₂ fixation to increase the algal productivity, such as *Chlorella sp.* (Hyun et al., 2008) and *Dunaliella tertiolecta* (Sydney et al., 2010).

Traditionally, microalgae are cultivated in closed systems or open ponds, which are aerated or exposed to air to allow microalgae to capture carbon dioxide from the atmosphere for cell growth. Industrial exhaust gases such as flue gas contains up to 15% CO₂ provide a CO₂-rich source for microalgal cultivation and a potentially cheap source for CO₂ bio-fixation. Therefore, it would be beneficial if microalgae are tolerant to elevated CO₂ level should they be used for CO₂ fixation from flue gases (Maeda et al., 1995). An early review on flue gas tolerance by microalgae indicated that high levels of CO₂ were tolerated by many microalgal species and that moderate levels of SO_x and NO_x (up to 150 ppm) were also well-tolerated (Matsumoto et al., 1997). However, the excess CO₂ leaving as unused gas to the atmosphere is the factor that should be considered and optimized CO₂ fed to the cultivation system.



Figure 2.3.2 *Physcomitrella patens* photobioreactor for biopharmaceutical (Eva, 2007)

2.4 CO₂ and bicarbonate as inorganic carbon source for microalgal uptake

Higher terrestrial plants usually depend entirely on CO₂ as their only source of inorganic carbon for photosynthesis, whereas marine microalgae acquire their inorganic carbon from the dissolved inorganic carbon (DIC) system in sea water. The DIC system contains four forms of carbon, i.e. CO₂, H₂CO₃, HCO₃⁻ and CO₃²⁻, their interconversion being governed by a complex equilibrium:



which is controlled primarily by pH and to a lesser degree by temperature and alkalinity (Merrett et al., 1996). Aquatic photosynthetic organisms face a number of problems in obtaining a supply of CO₂ for photosynthesis, causing largely from the physical chemistry of the water phase. The rate of diffusion of CO₂ in water is 1×10^4 times slower than it is in air, and at alkaline pH. HCO₃⁻ is the dominant dissolved inorganic carbon (DIC) species and the rate of spontaneous conversion of HCO₃⁻ to CO₂ is slow in this pH range. The low availability of CO₂ is particularly acute in seawater, which has a high ionic strength and an average pH of 8.0 to 8.2; most of the DIC (99%) is present in the form of HCO₃⁻ (about 2mM), whereas the CO₂ concentration is very low (10 mM at 20°C) (Round, 1981) and modeling of the diffusive CO₂ flux from the bulk phase to the plasmalemma suggests that the availability of CO₂ may be rate-limiting for the growth of marine diatoms (Riebesell et al., 1993).

Many photosynthetic microalgae achieve high photosynthetic rates via mechanisms that raise the intracellular CO₂ concentration (Kaplan and Reinhold, 1999). Many marine phytoplankton species possess a CO₂-concentrating mechanism (CCM), which consists of active CO₂ uptake, HCO₃⁻ uptake, and the presence of an external carbonic anhydrase (CA). Although it is not required for either CO₂ or HCO₃⁻ transportation, the presumed role of external CA is to maintain the CO₂/HCO₃⁻ equilibrium at the cell surface and thus ensure the availability of

substrate for the CO₂ transporter (Williams and Turpin, 1987). These microalgae can therefore acquire inorganic carbon by the direct uptake of bicarbonate or the active uptake of CO₂ derived from bicarbonate by the action of external CA.

A number of species have been found to display the characteristics of a CCM in that they have the capacity to accumulate inorganic carbon during photosynthesis. Leggat et al. (1999) showed a 7- to 26-fold accumulation over that in the external medium in *Amphidinium carterae* and a 5- to 24-fold accumulation in the symbiotic species *Symbiodinium sp.* A 10-fold accumulation has been reported in the marine species *Procentrum micans* (Nimer et al., 1999), and a 5- to 70-fold accumulation has been demonstrated in the freshwater species *Peridinium gatunense* (Berman-Frank et al., 1998). This capacity to accumulate inorganic carbon may be required to maintain photosynthetic CO₂ fixation.

At present, most ecophysiological studies of marine diatoms have focused on the ability of these organisms to take up macronutrients and trace metals and grow under various light regimes (Sarhou et al., 2005). By comparison, relatively few studies have examined the physiological mechanisms of inorganic C acquisition in this group. Early work suggested that the rate of diffusive CO₂ supply could significantly limit diatom growth as a result of the low CO₂ concentrations in marine surface waters and the poor CO₂ affinity of the principal RubisCO - carboxylating enzyme ribulose biphosphate carboxylase/oxygenase (RubisCO; Riebesell et al. 1993).

However, subsequent studies demonstrated the presence of inorganic carbon-concentrating mechanisms (CCMs) in a number of marine diatom species (Rotatore et al. 1995; Korb et al. 1997; Burkhardt et al., 2001; Morel et al., 2002). The CCM acts to concentrate CO₂ in close proximity to RubisCO via the active uptake of CO₂ and/or HCO₃⁻ (the dominant C form in seawater) and the use of carbonic anhydrase to catalyze the interconversion between these C species (Colman et al., 2002; Giordano et al., 2005).

There is a variety of inorganic carbon acquisition mechanisms in marine microalgae. Some have been shown to take up both CO₂ and HCO₃⁻ by active transport, with or without the involvement of an external CA (Colman and Rotatore 1995; Bozzo et al., 2000), whereas others have been found to take up only a single species of inorganic carbon (Rotatore et al. 1992,

Huertas and Lubian 1998; Huertas et al., 2000b). These algae therefore display all the combinations of inorganic carbon uptake that could be expected from the existence of two active inorganic carbon transporters and an external CA (Colman et al., 2002). The utilization of HCO_3^- may occur either by direct uptake or by CA catalysing the conversion of HCO_3^- to CO_2 and OH^- externally to the plasmalemma. Both mechanisms have been reported for marine macro- and microalgae. (Nimer and Merrett 1992; Dong et al., 1993)

2.5 Solubility of carbon dioxide in the water

As carbon dioxide causing the global warming, oceans represent in the largest carbon storage capacity in the world as a buffer. The natural uptake of CO_2 from the atmosphere by the ocean occurs on an enormous scale, and the ocean offers the world's most powerful long-term buffer against the rise of both temperature and CO_2 emissions (Brewer et al., 1995). Dissolved inorganic carbon in the ocean is increasing because of higher release of CO_2 to the atmosphere. Open ocean water in equilibrium with the atmosphere at 0°C contains about 2200 micromoles/liter CO_2 , which is about 75 times as much as that in fresh water and about 1% of the dissolved CO_2 in seawater is in the form of CO_2 (aqueous form) or H_2CO_3 , and 97% is in the form of HCO_3^- . Since the degree of ionic dissociation changes with pH, the solubility of CO_2 in seawater is a function of not only temperature but also pH (Round, 1981).

To enhance CO_2 capture and storage in the water, the solubility of CO_2 is essential to be understood and according to the occurring of mass transfer between gas and liquid phase, how CO_2 soluble in the water depends on these important factors influencing the gas solubility in the water i.e. (1) chemical property, (2) temperature and (3) pressure. Firstly, the solubility of one substance in another is determined by the balance of intermolecular forces between the solvent and solute, and the entropy change that accompanies the dissolution. The various characteristics of chemical substance e.g. polarity, enthalpy of formation and reactivity affect efficiently the solubility of gas in the liquid. Secondly, Due to the differences between gas and solid, solid substances are able to be dissolved well at higher temperature but contrary to the gas. Gas is dissolved better at lower temperature. As CO_2 solubility is temperature dependant, colder water

can dissolve more CO₂ and increasing water temperature reduces the solubility as demonstrated in Figure 2.5.1. Last, solubility is direct proportional to pressure so increasing in pressure causes more gas to dissolve in a liquid. At higher pressure, gas molecules are forced to be more dissolved into the liquid phase. Furthermore, Henry's law is commonly used to quantify the solubility of gases in solvents. The solubility of a gas in a solvent is directly proportional to the partial pressure of that gas above the solvent. This relationship is written as:

$$p = k_H c \quad (2.8)$$

where p is the partial pressure of the solute in the gas above the solution, c is the concentration of the solute and k_H is a constant with the dimensions of pressure divided by concentration

However, it should also be noted the use of Henry's Law is a limited only to low soluble gases, e.g. O₂ and N₂ where the solubility could be assumed to linearly vary with pressure. For relatively high soluble gases like CO₂, failure of Henry' law is observed because indirect proportion between solubility and pressure is often the case, and particularly for CO₂, the soluble CO₂ could undergo carbonation reaction leading to a formation of its carbonate derivatives like HCO₃⁻ and CO₃²⁻ according to the following reactions (Wilhelm et al., 1977):



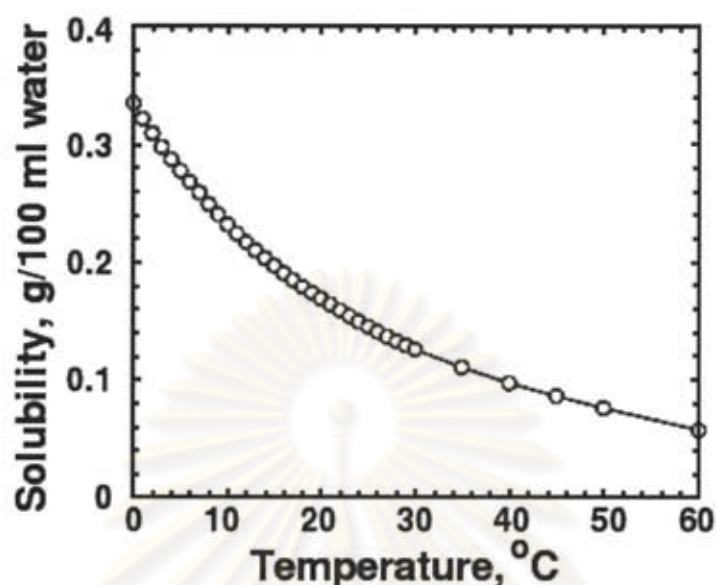
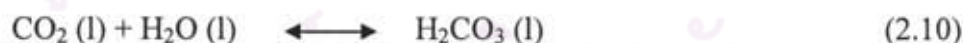


Figure 2.5.1 The relationship between solubility of CO_2 in the water (in $\text{g} \cdot 10^{-2} \text{ml}^{-1}$) at various temperature ($^{\circ}\text{C}$) at 1 atm pressure (Nielson, 2003)

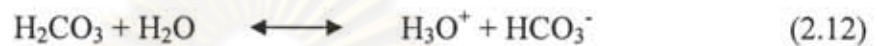
Any water-soluble gas becomes more soluble as the temperature decreases, due to the thermodynamics of the reaction, the entropy change, ΔS , of this reaction is positive because the gas molecules are less constrained than the gas molecules in solution. This effect is particularly large for gases like CO_2 that undergo specific reactions with water. Then, equilibrium is established between the dissolved CO_2 and H_2CO_3 , carbonic acid.



This reaction is kinetically slow. At equilibrium, only a small fraction (ca. 0.2 - 1%) of the dissolved CO_2 is actually converted to H_2CO_3 . Most of the CO_2 remains as solvated molecular CO_2 . As equation:

$$K_r = \frac{[\text{H}_2\text{CO}_3]}{[\text{CO}_2]_f} \approx 1.7 \cdot 10^{-3} \quad (2.11)$$

In fact, the pK_a (the symbol for the acid dissociation constant at logarithmic scale) most reported for carbonic acid ($pK_{a1} = 6.37$) is not really the true pK_a of carbonic acid. Rather, it is the pK_a of the equilibrium mixture of CO_2 (l) and carbonic acid. Carbonic acid is actually a much stronger acid than this, with a true pK_{a1} value of 3.58. However, these values are also temperature dependent (Wang et al., 2008). Carbonic acid is a weak acid that dissociates in following two steps (Lide et al., 1990):



which are controlled primarily by pH and alkalinity and described in interconversion of CO_2 in Equation (2.7) (Merrett et al., 1996).

Carbonate species are found in different pH range as shown in Figure 2.5.2. At high pH values, carbonic acid exists only in the form of carbonate ions. If the pH value decreases, the fraction of bicarbonate increases proportionally. At a pH around 10.3, both ions exist at equal amounts. Furthermore, low pH values, only bicarbonate exists at equilibrium. (Fleischer et al., 1998)

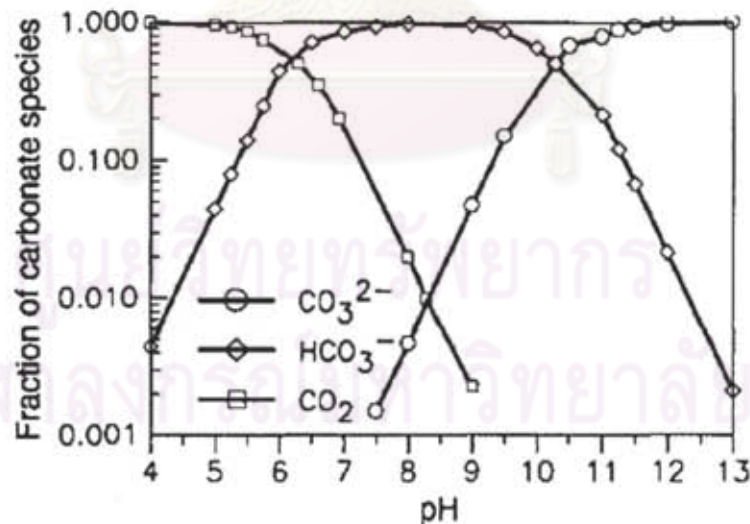


Fig 2.5.2 The various fraction of carbonate species in pH range from 4 to 13 (Fleischer et al., 1998)

2.6 Literature Review

From early twentieth century, Amine process using MEA (Monoethanolamine) as absorbent was found for CO₂ removal from pre-treated natural gas and then it was improved for removing CO₂ from coal-fired power plant and other purposes. However, MEA can cause energy penalty during absorption and regeneration cycle that relatively low temperature and high temperature are needed (described in Section 2.1). Furthermore, there are studies about alternative amine absorbent for substituting MEA e.g. NH₃ (ammonia) (Je et al., 2009; You et al., 2008; Bai et al., 2005; James et al., 2005; Yeh et al., 1999; Hsunling et al., 1997). Ammonia seems to be a promising alternative solvent for removing CO₂ from flue gas (Yeh et al., 1999).

From literature study, Amine processes using MEA and NH₃ in various important aspects e.g. fed CO₂ flow rate, flue gas composition, operating condition, maximum absorption capacity and averaged absorption rate were compared as shown in Table 2.6.1. MEA showed acceptable CO₂ absorption rate for commercial use. Furthermore, there was a study of chilled MEA (Temperature at -4°C) enhancing CO₂ removal (Yeh et al., 1999). However, it shows sign of energy penalty during cycle as mentioned above. Many NH₃ as absorbent studies were compared because NH₃ represents the better CO₂ capacity and absorption rate than MEA as shown in Table 2.6.1. The highest averaged absorption rate at room temperature and atmospheric pressure was presented at 12.01 kg CO₂·kg NH₃⁻¹·day⁻¹ (Je et al., 2009) and maximum absorption capacity at 0.98 kg of CO₂·kgNH₃⁻¹ (James et al., 2005). Moreover, chilled NH₃ process (at Temperature=-4°C) was also compared representing the highest maximum absorption capacity and averaged absorption rate at 1.20 kg of CO₂·kSg NH₃⁻¹ and 14.4 kg CO₂·kg NH₃⁻¹ day⁻¹ respectively (Yeh et al., 1999). This implied that temperature effect greatly yields better CO₂ absorption rate and capacity for NH₃ but considering energy penalty is required.

Table 2.6.1 Summary of CO₂ removal rate via amine processes

Absorbent	CO ₂ flowrate (l/min)	Flue gas composition (%v/v)	Absorbent concentration	Condition	Maximum Absorption Capacity	Averaged Absorption rate	Reference
NH ₃	2-10	40	7-35 %MEA, NH ₃	Temperature =-4 °C	1.20 kg CO ₂ kg NH ₃ ⁻¹	14.4 kg CO ₂ kg NH ₃ ⁻¹ d ⁻¹	Yeh et al., 1999
MEA	2-10			Pressure =101.3 kPa	0.40 kg CO ₂ kg MEA ⁻¹	4.80 kg CO ₂ kg MEA ⁻¹ d ⁻¹	
NH ₃	0.12	12.81	8.8 % NH ₃	Temperature =25°C Pressure =101.3 kPa	0.152 kg CO ₂ kg NH ₃ ⁻¹	7.30 kg CO ₂ kg NH ₃ ⁻¹ d ⁻¹	You et al., 2008
NH ₃	3	14.7	15 % NH ₃	Temperature =25°C Pressure =101.3 kPa	0.24 kg CO ₂ kg NH ₃ ⁻¹	11.52 kg CO ₂ kg NH ₃ ⁻¹ d ⁻¹	Bai et al., 2005
NH ₃	2	100	28 % NH ₃	Temperature = 25°C Pressure =101.3 kPa	0.9 kg of CO ₂ kg NH ₃ ⁻¹	10.8 kg CO ₂ kg NH ₃ ⁻¹ d ⁻¹	Hsunling et al., 1997
MEA	n/a	100	30 % MEA	Temperature = 25°C Pressure =101.3 kPa	0.36 kg of CO ₂ kg MEA ⁻¹	4.32 kg CO ₂ kg MEA ⁻¹ d ⁻¹	Jou et al., 1995
NH ₃	7.5	15	7-14 % NH ₃	Temperature =27 °C Pressure =101.3 kPa	0.98 kg CO ₂ kg NH ₃ ⁻¹	5.88 kg CO ₂ kg NH ₃ ⁻¹ d ⁻¹	James T. et al., 2005
NH ₃	20-30	25	2-7 % NH ₃	Temperature =25°C Pressure =101.3 kPa	0.252 kg CO ₂ kg NH ₃ ⁻¹	12.01 kg CO ₂ kg NH ₃ ⁻¹ d ⁻¹	Je et al., 2009

ศูนย์วิจัยและพัฒนา
จุฬาลงกรณ์มหาวิทยาลัย

CO₂ sequestration by photosynthetic organisms or autotrophs is being interesting throughout the world. Forestry, sea and fresh water plant are considered as alternative options for CO₂ removal. Because of highly potential growth rate of algae compared with other plants and some use CO₂ as their inorganic carbon for their growth. Furthermore, according to its substantial CO₂ removal benefit, captured CO₂ is completely transformed to biomass and some high-valued products. There are many studies on CO₂ for algal cultivation and global warming mitigation purposes. CO₂ fixation rates were compared in different living organisms and operating conditions as shown in Table 2.6.2. Literature recommends the range of condition for CO₂ fixation in the photobioreactors at: light intensity at range 40-250 $\mu\text{E m}^{-2} \text{s}^{-1}$ (Sydney et al., 2010; Hyun et al., 2008; de Morais et al., 2007; Yeoung et al., 1997; Kurano et al., 1995), various low to medium CO₂ flow rate at range 6.94-83.33 $\text{ml}\cdot\text{min}^{-1}$ (Eduardo et al. 2010; Hyun et al. 2008; de Morais et al., 2007), high CO₂ flow rate at range 400-1000 $\text{ml}\cdot\text{min}^{-1}$ (Yeoung et al., 1997; Kurano et al., 1995), different flue gas composition from 5 to 34 %v/v and a variety of mediums for algal cultivation were provided. Various algae are cultivated in fresh water and sea water in which they can naturally grow. Besides, Yeoung applied steel-making facility waste water for *Chlorella vulgaris* cultivation as substituted nutrients in which high value CO₂ fixation ($0.624 \text{ g l}^{-1}\text{d}^{-1}$) was taken (Yeoung et al., 1997). If only fresh water or artificial sea water are considered without pH effect, Sea water *Chlorococcum Littora* represents the highest CO₂ fixation among other sea water algae at $0.900 \text{ g l}^{-1}\text{d}^{-1}$ (Kurano et al., 1995) and fresh water *Chlorella sp.* shows the second highest CO₂ fixation at $0.570 \text{ g l}^{-1}\text{d}^{-1}$. Note that in many cases, CO₂ supplied to algal culture is wasted to the atmosphere as CO₂ consumption rate at which the alga can uptake is relatively low.

From Tables 2.6.1 and 2.6.2, CO₂ removal via amine process and algal cultivation can be compared in many diverse aspects, e.g. CO₂ removal rate per day, chemical utilization and unit operation. CO₂ removal rate per day in amine process representing in averaged absorption rate (in $\text{kg CO}_2 \text{ kg absorbent}^{-1} \text{ day}^{-1}$) are clearly better than in algal cultivation (in $\text{g l}^{-1}\text{d}^{-1}$). Nevertheless, amine process costs a chemical expenditure and need energy provided for absorption and regeneration cycle via costly absorber and desorber columns. On the contrary,

CO₂ removal via algal cultivation requires little chemical for medium, no need for regeneration cycle and reacted CO₂ is completely transformed into biomass by simple photobioreactors. Eventually, Amine process is still reliable and effective for industrial scale use and CO₂ removal via algal cultivation need to be more improved for competitive CO₂ removal for substantial development.



ศูนย์วิทยทรัพยากร
จุฬาลงกรณ์มหาวิทยาลัย

Table 2.6.2 Summary of CO₂ removal rate via algal cultivation

Microalgae	Reactor type / volume	Condition	CO ₂ rate (ml/min)	Flue gas Composition (%v/v)	CO ₂ fixation (g l ⁻¹ d ⁻¹)	Remark	Reference
<i>Chlorella vulgaris</i>	Photobioreactor / 0.25 l	Temperature = 27 °C Medium : N8 Medium Light intensity = 110 μE m ⁻² s ⁻¹	400	15	0.624	Using suspended solid removed wastewater from steel-making facility	Yeoung et al., 1997
<i>Haematococcus pluvialis</i>	Photobioreactor / 180 l	Temperature = 16-18 °C Medium : n/a Light intensity >2200 μE m ⁻² s ⁻¹	n/a	16-34	0.143	Commercial scale, outdoor and using daylight Addition of CO ₂ until pH in range of 7.3-7.8	Huntley et al., 2007
<i>Spirulina sp.</i>	Photobioreactors (3)/ total volume 5.4 l	Temperature = 30 °C Medium : modified Zarrouk medium Light intensity = 43.24 μE m ⁻² s ⁻¹	55.56	12	0.413	-	de Morais et al., 2007
<i>Chlorella sp.</i>	Photobioreactors (4)/ total volume 2.4 l	Temperature = 20 °C Medium : Allen medium Light intensity = 40 μE m ⁻² s ⁻¹	83.33	5	0.570	-	Ryu et al., 2008
<i>Botryococcus braunii</i>	Photobioreactor / 8 l	Temperature = 25 °C Medium : 3N-MBM medium Light intensity = 47.30 μE m ⁻² s ⁻¹	6.94	5	0.500	Artificial sea water pH 7.2±0.2 adjusted by acid/base injection	Sydney et al., 2010
<i>Spirulina platensis</i>	Photobioreactor / 8 l	Temperature = 30 °C Medium : Zarrouk medium Light intensity = 47.30 μE m ⁻² s ⁻¹	6.94	5	0.320	Artificial sea water pH 9.0±0.2 adjusted by acid/base injection	Sydney et al., 2010
<i>Dunaliella tertiolecta</i>	Photobioreactor / 8 l	Temperature =25 °C Medium : DUN medium Light intensity = 47.30 μE m ⁻² s ⁻¹	6.94	5	0.270	Artificial sea water pH 7.2±0.2 adjusted by acid/base injection	Sydney et al., 2010
<i>Chorella. vulgaris</i>	Photobioreactor / 8 l	Temperature = 30 °C Medium : modified Britol medium Light intensity = 47.30 μE m ⁻² s ⁻¹	6.94	5	0.250	Artificial sea water pH 7.2±0.2 adjusted by acid/base injection	Sydney et al., 2010
<i>Chlorococcum Littora</i>	Culture vessel / 20 l	Temperature = 25 °C Medium : Allen medium Light intensity = 250 μE m ⁻² s ⁻¹	1000	6.25	0.900	Artificial sea water pH was not adjusted	Kurano et al., 1995

CHAPTER III

MATERIALS AND METHODS

Experimental methods can be divided into two parts; (1) maximising CO₂ dissolution in bubble column, and (2) the usage of bicarbonate as inorganic carbon source for fresh water microalgae *Chlorella vulgaris*. The first and second parts are illustrated in Figures 3.1 and 3.2, respectively. For CO₂ dissolution study, many manipulated variables are examined and then finally evaluated for the optimal dissolution condition. This can be elucidated using Figure 3.1. Figure 3.2 displays the details of experiments in which bicarbonate is employed as inorganic carbon source for fresh water microalgae cultivation. *C. vulgaris* is chosen to be the fresh water algal model in this work due to its rapid growth rate and ease of system maintenance.

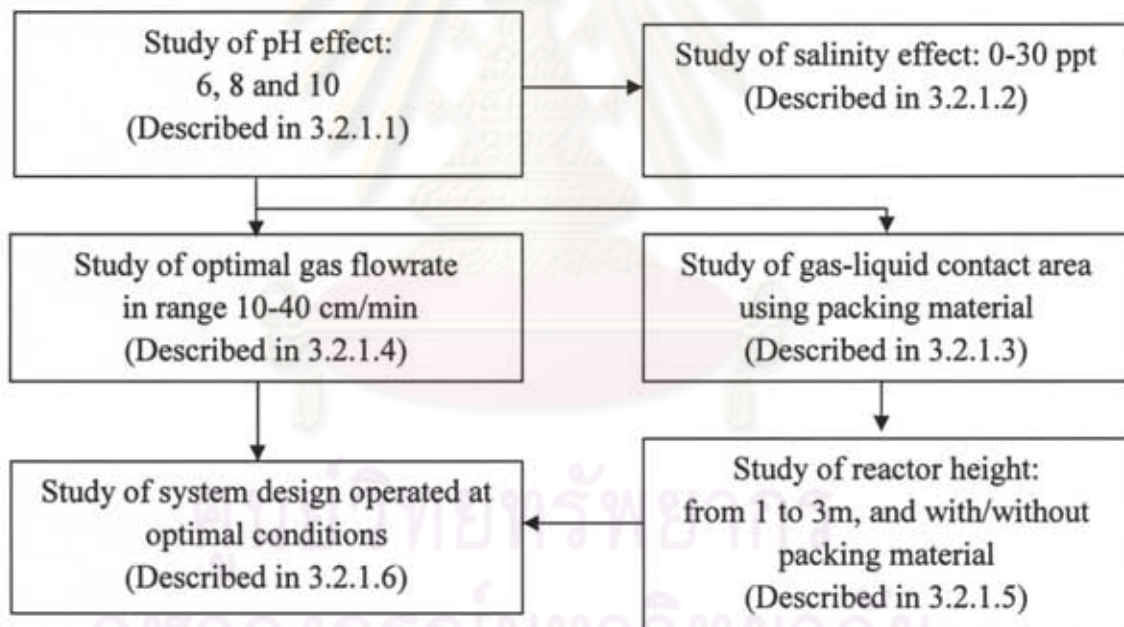


Figure 3.1 Experimental diagram: Maximising CO₂ dissolution in bubble column

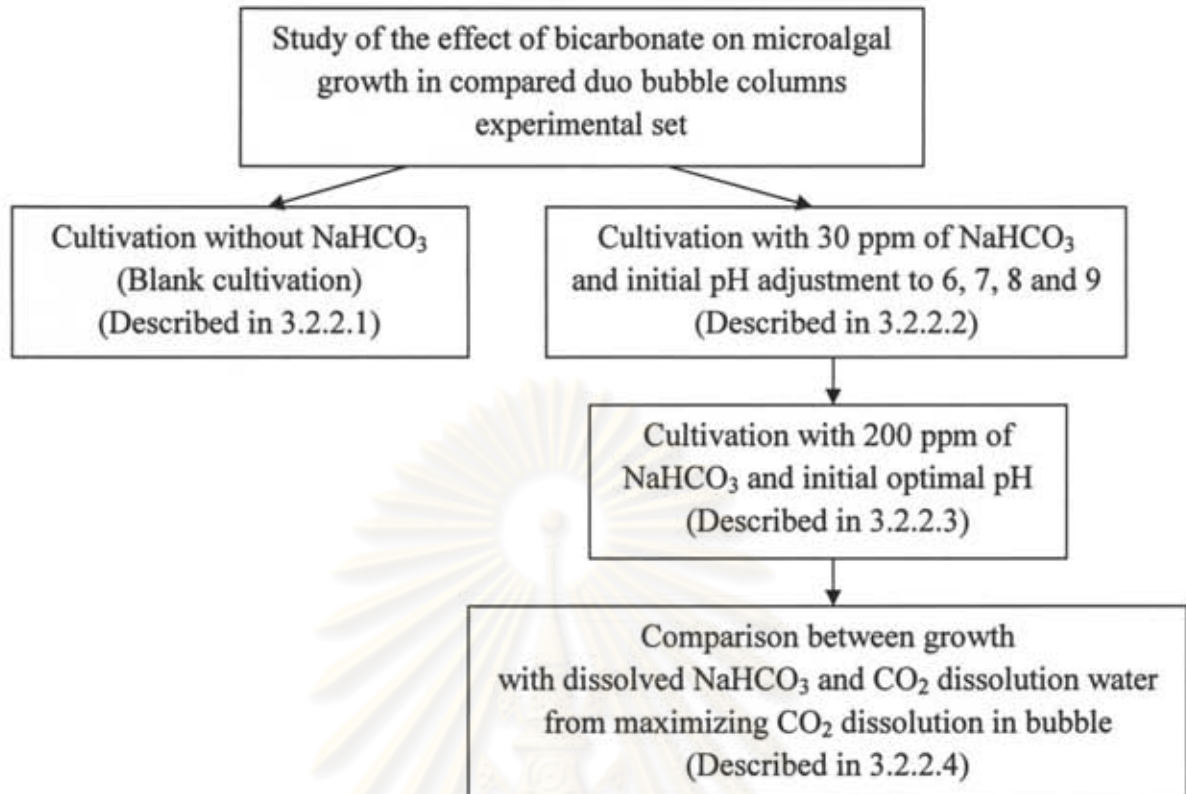


Figure 3.2 Experimental diagram: Study of bicarbonate as inorganic carbon source for fresh water microalgae cultivation

3.1 Experimental Setup

3.1.1 Combined effect of system design for CO₂ dissolution

3.1.1.1 Experiments in bubble columns

The effect of pH and salinity on CO₂ dissolution in the water is investigated in a 1 m high clear acrylic plastic bubble column with a diameter of 6.3 cm (see Fig. 3.3 for a schematic of the bubble column). In case of study of optimal gas flowrate, 2 metre high bubble column with the same diameter is instead employed. CO₂ gas is fed from gas cylinder and measured with a “Dawyer” rotameter before entering the reactor at the bottom. The gas velocity is controlled and sparged at 10 cc min⁻¹.

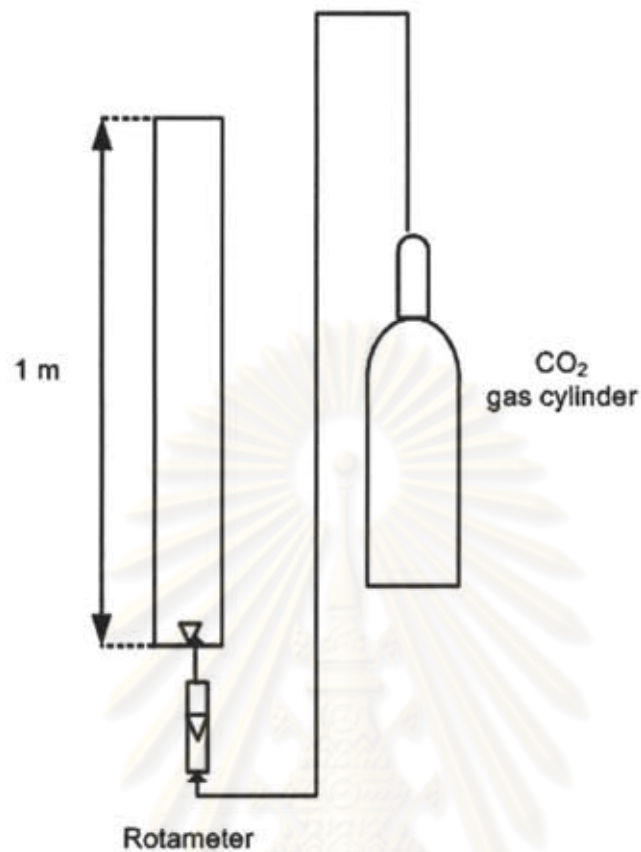


Figure 3.3 Experimental setup for CO₂ fed bubble column

3.1.1.2 Experiments in packed columns

The effect of gas-liquid contact area on CO₂ dissolution is studied in a 1 m high clear acrylic plastic bubble column. This is exactly the same column as that used in Section 3.1.1.1 but this time fully filled with 1 cm diameter packing material. In case of study effect of height in packed material, 3 metre high packed column with equal diameter is replaced. CO₂ gas is fed from gas cylinder and measured with a “Dawyer” rotameter before entering the reactor at the bottom. The gas velocity is controlled and sparged at 10 cc min⁻¹.



Figure 3.4 One cm diameter packing material

3.1.1.3 Circulating Counterflow Contactor (C.C.C.) packed column

The combined effect of system design for optimal CO₂ dissolution is investigate in “C.C.C” in which 1 m high packed column is fully filled with packing material. Water is allowed to circulate in transverse direction with gas fed (see Fig.3.4). Water recycle flowrate is manipulated with rotameter at a desire range of 1-3 LPM (Litres per minute). Submerged pump is placed in 5 Litres reservoir enabling water to circulate further. CO₂ gas is fed from gas cylinder and measured with a “Dawyer” rotameter before entering the reactor at the bottom. The gas velocity is controlled and sparged at 10 cc min⁻¹.

ศูนย์วิทยทรัพยากร
จุฬาลงกรณ์มหาวิทยาลัย

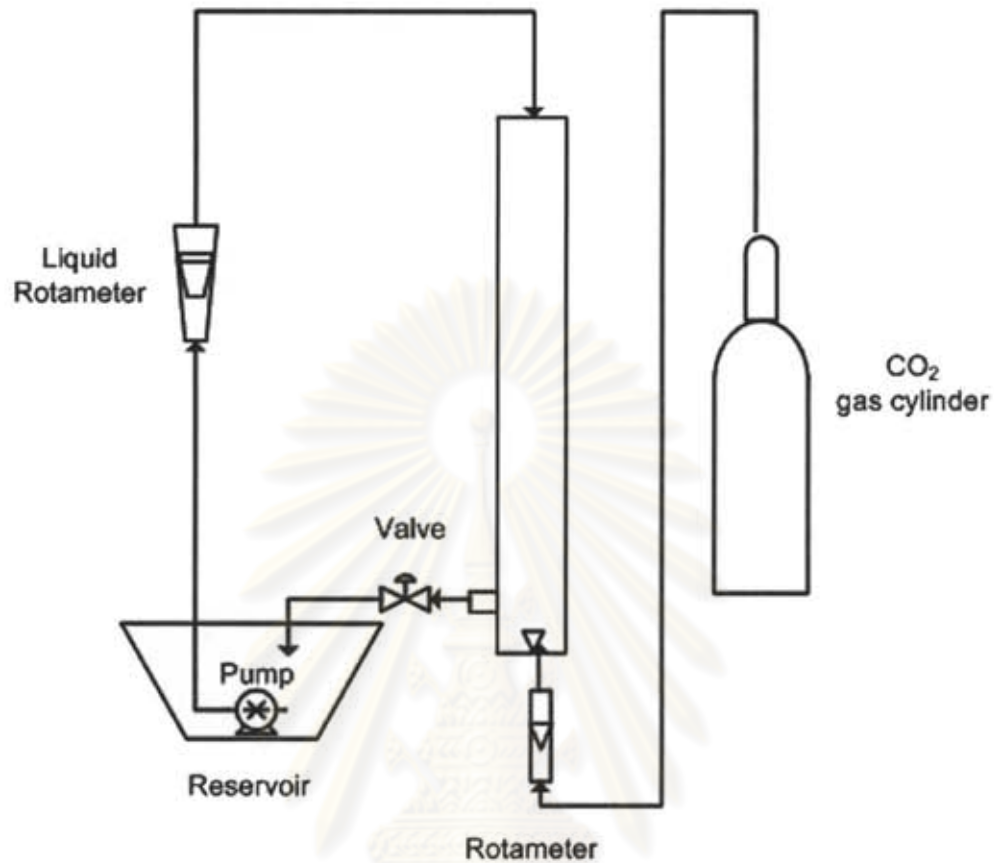


Figure 3.5 Experimental setup for Circulating Counterflow Contactor

3.1.2 Effect of bicarbonate as inorganic carbon source for fresh water microalgae

Two 2.8 L bubble columns are prepared side by side to allow the sharing of light source as illustrated in Fig 3.4. This system is thereafter called “duo bubble columns”. 18 W Fluorescent light bulbs are located between the two columns illuminating 10000 Lux light intensity. Fresh water is sterilised by 50 ppm (parts per million) of chlorine (as sodium hypochloride), air is measured with “Dawyer” rotameter and supplied at a superficial velocity (U_{sg}) = 1 cm/s.

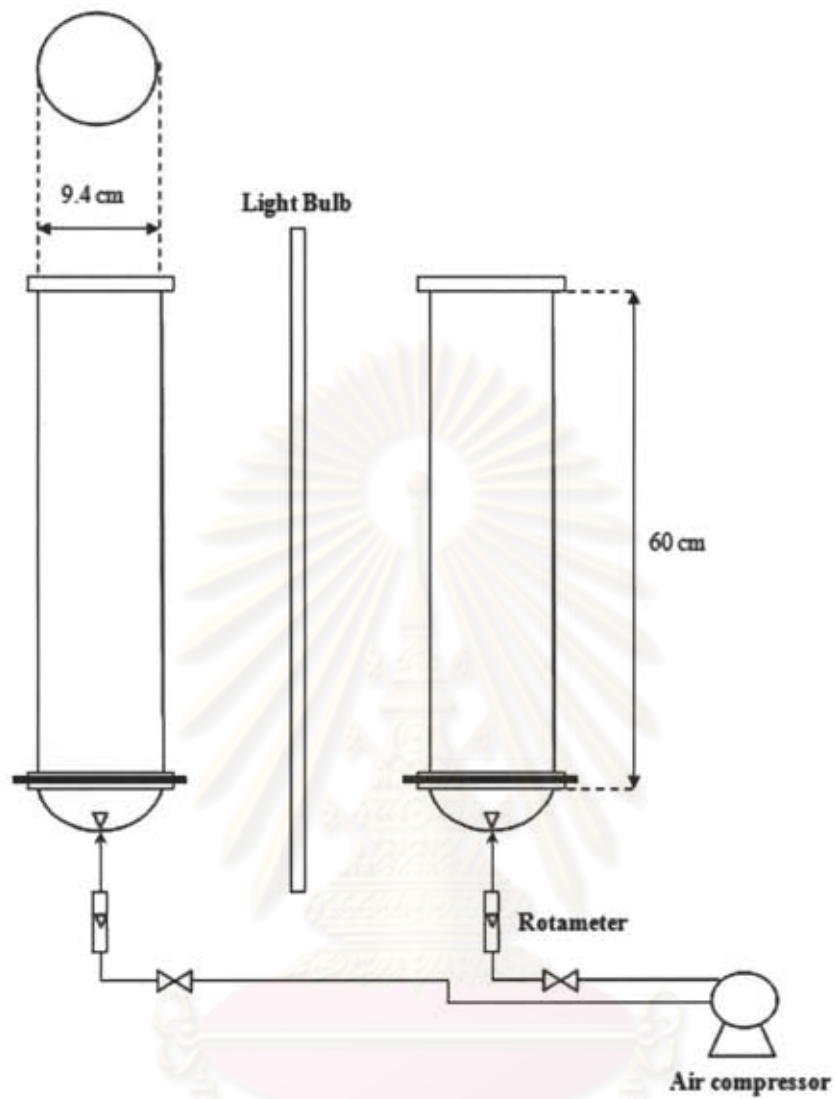


Figure 3.6 Experimental setup for cultivation of *Chlorella vulgaris* in sharing light source bubble columns

จุฬาลงกรณ์มหาวิทยาลัย

3.2 Experimental Procedure

3.2.1 Maximising CO₂ dissolution in bubble column

3.2.1.1 Study of pH effect

1. Setup the sparged bubble column as described in Section 3.1.1.1
2. Adjust demineralised water with HCl 0.5 M and NaOH 0.5 M at pH of 6, 8 and 10.
3. Sparge CO₂ from the gas cylinder to the porous sparger at the bottom of the column.
4. Collect 20 ml sample at every 15 minutes for one hour; store the collected samples in refrigerator.
5. Analyse for Total Inorganic Carbon (TIC) by using Shimadzu Total Inorganic Carbon (TOC) Analyser

3.2.1.2 Study of salinity effect

1. Setup the sparged bubble column as described in Section 3.1.1.1
2. Replace fresh water with sea water at salinity of 5, 10 and 30 ppt
3. Sparge CO₂ from the gas cylinder to the porous sparger at the bottom of the column.
4. Collect 20 ml at every 15 minutes for one hour; store the collected samples in refrigerator.
5. Analyse for Total Inorganic Carbon (TIC) by using Shimadzu Total Inorganic Carbon (TOC) Analyser

3.2.1.3 Study of gas-liquid contact area effect

1. Setup the sparged packed column as described in Section 3.1.1.2
2. Adjust demineralised water with HCl 0.5 M and NaOH 0.5 M at pH of 6, 8 and 10.
3. Sparge CO₂ from the gas cylinder to the porous sparger at the bottom of the column.
4. Collect 20 ml at every 15 minutes for one hour; store the collected samples in refrigerator.
5. Analyse for Total Inorganic Carbon (TIC) by using Shimadzu Total Inorganic Carbon (TOC) Analyser

3.2.1.4 Study of optimal gas flowrate effect

1. Setup the sparged packed column as described in Section 3.1.1.2
2. Adjust demineralised water at optimal pH obtained from Section 3.2.1.1 with HCl 0.5 M and NaOH 0.5 M
3. Sparge CO₂ at 10, 20, 30 and 40 from the gas cylinder to the porous sparger at the bottom of the column.
4. Collect 20 ml at every 15 minutes for one hour; store the collected samples in refrigerator.
5. Analyse for Total Inorganic Carbon (TIC) by using Shimadzu Total Inorganic Carbon (TOC) Analyser

3.2.1.5 Study of height and gas-liquid contact area effect

1. Setup the sparged packed column as described in Section 3.1.1.2
2. Adjust demineralised water with NaOH 0.5 M and HCl 0.5 M at optimal pH from obtained Section 3.2.1.1
3. Sparge CO₂ from the gas cylinder to the porous sparger at the bottom of the column.
4. Collect 20 ml at every 15 minutes for one hour; store the collected samples in refrigerator.
5. Analyse for Total Inorganic Carbon (TIC) by using Shimadzu Total Inorganic Carbon (TOC) Analyser

3.2.1.6 Study of combined effect of optimal conditions

This experiment employs the combined optimal conditions obtained from Sections 3.2.1.1-3.2.1.5 in order to determine the best condition for CO₂ dissolution in the bubble column.

1. Setup the sparged bubble column as described in Section 3.1.1.3
2. Adjust demineralised water with NaOH 0.5 M and HCl 0.5 M at optimal pH obtained from Section 3.2.1.1
3. Manipulate the recycle water flowrate at 1, 2 and 3 LPM
4. Sparge CO₂ from the gas cylinder to the porous sparger at the bottom of the column.

5. Collect 20 ml at every 15 minutes for one hour; store the collected samples in refrigerator.
6. Analyse for Total Inorganic Carbon (TIC) by using Shimadzu Total Inorganic Carbon (TOC) Analyser

3.2.2 Effect of bicarbonate on microalgal growth

Study of bicarbonate and pH effect on microalgal, *Chlorella vulgaris* growth can be divided into 4 experiments; 3.2.2.1 Blank cultivation (controlled experiment) –no bicarbonate added and no pH adjustment, 3.2.2.2 Cultivation with 30 ppm of NaHCO_3 and pH adjustment in range of 6-9, 3.2.2.3 Cultivation with 200 ppm of NaHCO_3 at optimal pH from 3.2.2.2, and finally 3.2.2.4 cultivation with the medium prepared from the Section 3.2.1.5 (with CO_2 dissolution). Next, 3.2.2.1-3.2.2.3 experiments are initially conducted by this followings.

1. Setup the bioreactors as described in Section 3.1.2
2. Sterilise the duo bubble columns and fresh water with 50 ppm chlorine (as sodium hypochloride). Sparge air through the porous sparger at the bottom of the column for about 1 day. Check the residual chlorine in fresh water by adding potassium iodide in fresh water, and if chlorine is not exhausted, the sample will be turned yellow.
3. Fill the column with sterilised culture medium together with pure culture with initial cell concentration of 1×10^6 cells mL^{-1} and adjust the total working volume to 2.8 L
4. Supply the compressed air through a porous sparger and adjust the superficial gas velocity to 1 m s^{-1}

5. Supply both sides of column with 18 W fluorescent light bulbs, placed along the column height. The light intensity is adjusted in the range of 9,000 – 10,000 luxes or $122\text{-}136 \mu\text{mol photon m}^{-2}\text{s}^{-1}$ by moving the light bulbs in or out from the column as shown in Figure 3.5.
6. Further experiment method for different conditions will be described in 3.2.2.1, 3.2.2.2 and 3.2.2.3.

3.2.2.1 Cultivation of *Chlorella vulgaris* without NaHCO_3 added and pH adjustment

1. Set up bioreactor as described in 3.2.2
2. Take samples daily and count for the cell density using Haemocytometer (mentioned in Section 3.3.2).
3. Calculate the specific growth rate using Equation 3.3

3.2.2.2 Effect of bicarbonate and pH on microalgal growth

1. Setup bioreactor as described in 3.2.2
2. Setup $30 \text{ mg}\cdot\text{L}^{-1}$ bicarbonate concentration in both reactors by adding dried NaHCO_3 .
3. Adjust pH to 6, 7, 8 and 9 in both reactors by acid/base injection; NaOH 0.5 M and HCl 0.5 M
4. Take samples daily and count for the cell density using Haemocytometer (mentioned in Section 3.3.2).

5. Calculate the specific growth rate using Equation 3.3, the productivity using Equation 3.4 and the specific productivity using Equation 3.5

3.2.2.3 Effect of 200 ppm of NaHCO₃ on microalgal growth

1. Setup bioreactor as described in 3.2.2
2. Setup 200 mg·L⁻¹ bicarbonate concentration in both reactors by adding dried NaHCO₃
3. Adjust pH to optimal pH (obtained from 3.2.2.2) in both reactors by acid/base injection; NaOH 0.5 M and HCl 0.5 M
4. Take samples daily and count for the cell density using Haemocytometer (mentioned in Section 3.3.2).
5. Calculate the specific growth rate using Equation 3.3, the productivity using Equation 3.4, and the specific productivity using Equation 3.5

3.2.2.4 Effect of CO₂ dissolution water from optimal combined effect bubble column

1. Setup the bioreactors as described in Section 3.1.2
2. Sterilize the duo bubble columns with 50 ppm chlorine (as sodium hypochloride). Sparge air through the porous sparger at the bottom of the column for about 1 day. Check the residual chlorine in fresh water by adding potassium iodide in fresh water, and if chlorine is not exhausted, the sample will be turned yellow.

3. Release the sterilized water from the bioreactor.
4. Fill the column with CO₂ dissolution water from 3.2.1.5
5. Fill the column with sterilized culture medium together with the pure culture with initial cell concentration of 1×10^6 cells mL⁻¹ and adjust the total working volume to 2.8 L
6. Supply the compressed air through a porous sparger and adjust the superficial gas velocity to 1 m s⁻¹
7. Supply both sides of column with 18 W fluorescent light bulbs, placed along the column height. The light intensity is adjusted in the range of 9,000 – 10,000 luxes or 122-136 $\mu\text{mol photon m}^{-2}\text{s}^{-1}$ by moving the light bulbs in or out from the column as shown in Figure 3.5.
8. Adjust pH to optimal pH from 3.2.2.2 experiment in both reactors by acid/base injection; NaOH 0.5 M and HCl 0.5 M
9. Take samples daily and count for the cell density using Haemocytometer (mentioned in Section 3.3.2).
10. Calculate the specific growth rate using Equation 3.3, the productivity using Equation 3.4 and the specific productivity using Equation 3.5

3.3 Analyses

3.3.1 Determination of Total Inorganic Carbon (TIC)

Dissolved inorganic carbon (DIC) is the sum of inorganic carbon species in a solution. The inorganic carbon species include carbon dioxide, carbonic acid, bicarbonate anion, and carbonate. It can express carbon dioxide and carbonic acid simultaneously as

CO_2^* . C_T is a key parameter when making measurements related to the pH of natural aqueous systems, and carbon dioxide flux estimates.

$$C_T = [\text{CO}_2^*] + [\text{HCO}_3^-] + [\text{CO}_3^{2-}]$$

where,

C_T is the total inorganic carbon concentration ($\text{mg}\cdot\text{L}^{-1}$)

$[\text{CO}_2^*]$ is the sum of carbon dioxide and carbonic acid concentrations
($[\text{CO}_2^*] = [\text{CO}_2] + [\text{H}_2\text{CO}_3]$) ($\text{mg}\cdot\text{L}^{-1}$)

$[\text{HCO}_3^-]$ is the bicarbonate concentration ($\text{mg}\cdot\text{L}^{-1}$)

$[\text{CO}_3^{2-}]$ is the carbonate concentration ($\text{mg}\cdot\text{L}^{-1}$)

Total inorganic carbon is determined by Acidification of phosphoric acid operating in removal and venting of IC and POC (Particulate Organic Carbon) gases from the liquid. Then, IC mostly transforms into CO_2 and it is detected by the non-dispersive infrared analysis (NDIR). A region of adsorption of infrared light specific to CO_2 , usually around $4.26 \mu\text{m}$ (2350 cm^{-1}), is measured over time as the gas flows through the detector. The gas continues to flow into and out of the detector cell, the sum of the measurements results in a peak that is integrated and correlated to the total CO_2 concentration or Total Inorganic carbon totally found in the sample, in concentration, mg/l .

3.3.2 Determination of % CO_2 dissolution efficiency

%Efficiency of CO_2 dissolution for each time can be determined from proportion of CO_2 dissolved as TIC in mg divided by the total amount of CO_2 entering the reactor in mg :

$$\%Efficiency = \frac{TIC \times V_L}{\left(\frac{PQ_g t M_w}{RT}\right)} \quad (3.1)$$

where

TIC = Total Inorganic Carbon concentration ($\text{g}\cdot\text{L}^{-1}$)

V_L = Volume of water in bubble or packed column (L)

P = Pressure (bar)

Qg = Volumetric flowrate of CO_2 fed in the system ($\text{L}\cdot\text{min}^{-1}$)

t = Time operated (min)

Mw = Molecular weight ($\text{g}\cdot\text{mol}^{-1}$)

R = Gas constant = $82 \text{ bar}\cdot\text{L}\cdot\text{mol}^{-1}\cdot\text{K}^{-1}$

T = Temperature (K)

3.3.3 Determination of cell concentration

Due to the very high density of *Chlorella sp.*, appropriate dilution is needed. Cell concentration is determined using Haemocytometer. The depth of the counting grid and the medium area are 0.1 mm and 0.04 mm^2 , respectively. The cell concentration can be determined as follows:

1. Clean the counting slide and cover glass
2. Fill the slide with sample
3. Cover the slide with cover glass, avoid the presence of bubbles
4. Count the cell in 25 medium squares on the grid

5. Calculate the cells number, using Equation 3.2:

$$N = \frac{n}{25} \times 10^5 \quad (3.2)$$

where

N = cells concentration (cells·mL⁻¹)

n = number of cells on 25 squares in upper and lower grid (cells)

3.3.4 Determination of specific growth rate

The specific growth rate can be calculated from Equation 3.3 as follows:

$$\mu = \frac{\ln(N_2) - \ln(N_1)}{t_2 - t_1} \quad (3.3)$$

where

μ = specific growth rate (h⁻¹)

N_1 = cells concentration at t_1 (cells·mL⁻¹)

N_2 = cells concentration at t_2 (cells·mL⁻¹)

t_1 = first sampling time (h)

t_2 = second sampling time (h)

CHAPTER IV

Results and Discussion

4.1 Maximising CO₂ dissolution in bubble column

4.1.1 Effect of pH on total inorganic carbon dissolved in the water

pH in the range of 6 to 10 were chosen to study its effect on CO₂ dissolution in the water because bicarbonate species can be found in this range as dissolved inorganic carbon and, in many cases, suits to be fed into cultivation systems as inorganic carbon source for microalgal growth. Figure 4.1.1 illustrates the time profiles of Total Inorganic Carbon (TIC) measured from TOC analyser in the unit of milligram per litre (mg·L⁻¹) at all pH range. During the course of the experiment (from 0 to 60 minutes), the total dissolved inorganic carbon increased steadily with time and accumulated in the bubble column. The maximum dissolution at pH 10 (measured from the total inorganic carbon) was most of the time higher than those obtained at pH 6 and 8. In fact, pH 6 saw the lowest trend of CO₂ dissolution.

From Table 4.1.1, CO₂ dissolution efficiencies (proportion of CO₂ dissolved as TIC in mg divided by the total amount of CO₂ entering the reactor in mg) achieved the highest and lowest at pH 10 and 6, respectively. At the beginning of the experiment, inorganic carbon was able to dissolve quite rapidly in the liquid, but the dissolving rate decreased subsequently. The highest efficiency of 49.81% was obtained at the beginning of experiment with pH 10 (15th minutes). The high efficiency at early stage could be due to the high concentration difference driving force (ΔC) as described in the following mass transfer rate equation:

$$N = kA\Delta C \quad (4.1)$$

where	N	=	Mass transfer rate ($\text{g}\cdot\text{min}^{-1}$)
	k	=	Mass transfer coefficient ($\text{m}\cdot\text{min}^{-1}$)
	A	=	Mass transfer area (m^2)
	ΔC	=	Concentration difference ($\text{g}\cdot\text{m}^{-3}$)

(Note: $\Delta C = \text{Equilibrium liquid phase concentration } (\overline{C_g}) - \text{Liquid phase concentration } (C_l)$ where $\overline{C_g}$ is assumed to be the liquid phase concentration which is in equilibrium with gas phase concentration (C_g)).

At the beginning, the concentration of inorganic carbon in liquid was very low compared with the equilibrium concentration ($\overline{C_g} \gg C_l$). As the result, high mass transfer rate was observed and this is reflected in the apparent high %efficiency of CO_2 dissolution. At later stage, the dissolved CO_2 (C_l) became high, lowering the concentration difference (ΔC), and so did the mass transfer rate. At sufficient contacting time, C_l reaches approximately the equilibrium liquid phase concentration ($\overline{C_g}$) resulting in $\Delta C \rightarrow 0$ and no further net mass transfer would take place. Fortunately, CO_2 could undergo chemical transformation to bicarbonate and carbonate according to Equation (4.2) and therefore this maintained the liquid phase CO_2 concentration at a lower level than the equilibrium concentration. Consequently, the gas-liquid mass transfer could continue according to the level of ΔC driving force at that particular moment.

The change in pH could manipulate the rate at which CO_2 transforms to bicarbonate and carbonate. Experiment demonstrates that at high pH, this transformation occurred at a more rapid rate. In other words, high pH level or high degree of alkalinity leads to the forward reactions (2) and (3) in Equation (4.2). As the result, a low ΔC for CO_2 could be maintained at a longer period and a high level of CO_2 dissolution could consequently be obtained. It was demonstrated in this section that an increase in pH could lead to a greater dissolution of CO_2 resulting in a greater TIC concentration trend. Within the range of pH investigated, pH 10 gave

the highest fraction of inorganic carbon being dissolved in the liquid compared with other pH levels.

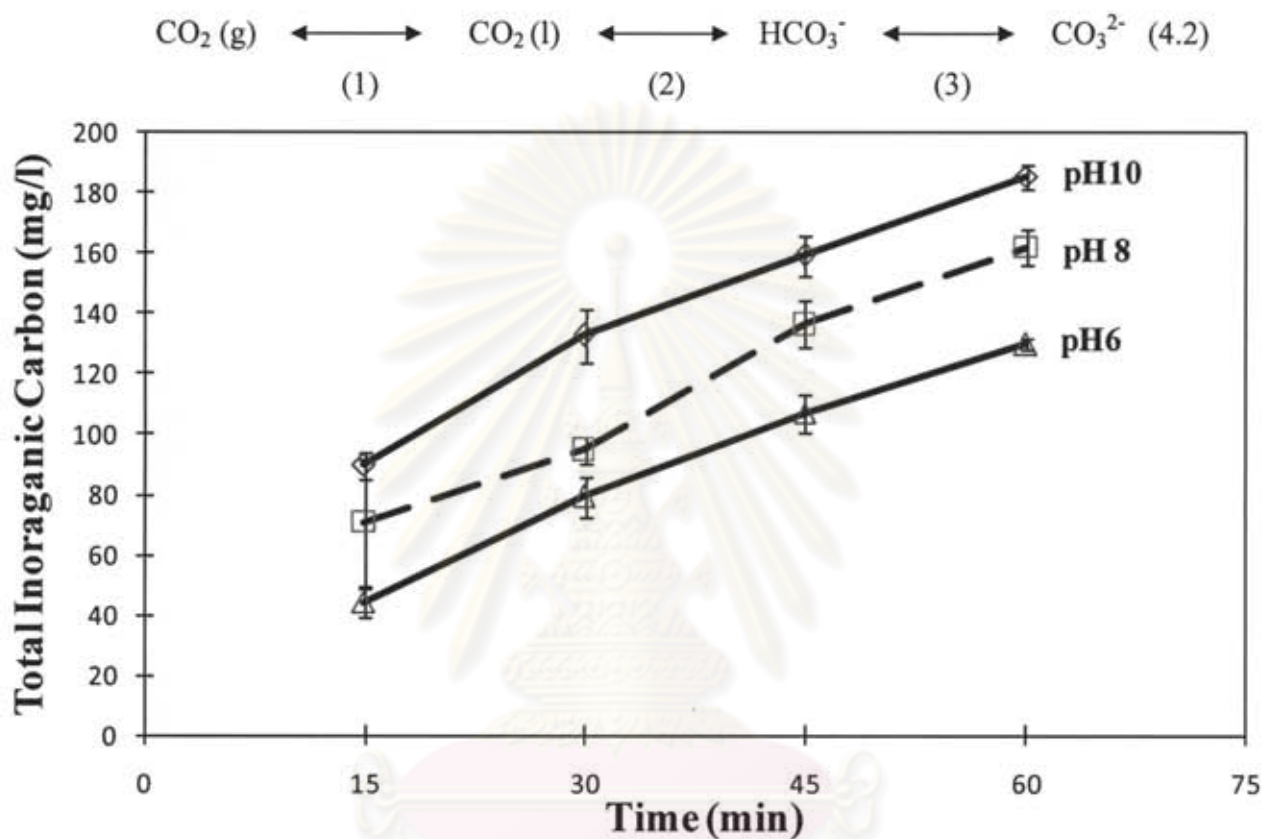


Figure 4.1.1 Total Inorganic Carbon time profile at various pH levels

ศูนย์วิทยทรัพยากร
 จุฬาลงกรณ์มหาวิทยาลัย

Table 4.1.1 % Efficiency of CO₂ dissolution at various pH levels

Time (min)	%Efficiency (Carbon Balance)		
	pH 6	pH 8	pH 10
15	22.26	35.83	45.28
30	20.00	23.92	33.41
45	17.98	22.91	26.76
60	16.35	20.42	23.38

4.1.2 Effect of gas-liquid contacting area on total inorganic carbon dissolved in the water

In this section, packing material was fully packed in 1 m high bubble column to enhance the contacting area between gas and liquid. Although the effect of pH on TIC dissolved in the water was already reported in the previous section, the different configured columns were operated at the various pH levels (at 6, 8 and 10) to ensure that there is no relationship between the two effects. In addition, samples were collected at different heights, at the middle and top of the column. Distinctly, TIC time profile in Figure 4.1.2.1(a) representing the concentration at the top part of the column displayed the highest TIC trend at pH 10. In contrast, pH 6 showed the lowest TIC trend compared with the others which confirms the effect of pH as discussed earlier. Similarly, the highest TIC as shown in Figure 4.1.2.1(b) was achieved at pH 10. Note that there were not much differences between the results at pH 6 and pH 8, and from hereafter, only the results at pH 10 will be discussed unless otherwise mentioned. The highest efficiency, 51.87% at pH 10, was reported at middle of the column as reported in Table 4.1.2. %Efficiency largely decreased with time, e.g. 51.87% at 15th min and then, 35.33% at 30th min because of lower mass transfer rate due to the increase of C_1 over time as described in

previous section. At the beginning of experiment, at lower position of column, equilibrium liquid phase concentration ($\overline{C_g}$) was largely higher than concentration in liquid (C_l) which resulted in higher %efficiency in CO_2 dissolution at the middle compared with at the top of the column. At a longer time period (30th min and later), not much differences in %efficiency at the top compared with the middle were observed because the influential factor in concentration difference decreased with time.

The effect of gas-liquid on TIC dissolved at pH 10 in different contactor configurations, i.e. bubble and packed column, is illustrated in Figure 4.1.2.2. Adding gas-liquid contacting area (by introducing the packing material) led to a higher rate of CO_2 dissolved in the water. Gas hold up (ϵ_g) is calculated by the following equation:

$$\epsilon_g = \frac{V_g}{V} \quad (4.3)$$

where

$$\begin{aligned} \epsilon_g &= \text{Gas holdup} \\ V_g &= \text{Volume of gas in the column (L)} \\ V &= \text{Volume of liquid in the column (L)} \end{aligned}$$

$\epsilon_{g,b}$ and $\epsilon_{g,p}$ are equal to 1.1 and 2.3 for the 1m high bubble column and 1 m high packed column, respectively (see Appendix C.2). This means that, provided that the bubble size remained unaltered, using packing material could enhance the gas holdup significantly and this led to a higher contacting area. Proportionally, having a 2 times higher gas holdup, the contacting area was expected to also be two times higher in the packed column than in the bubble column. However, the mass transfer rate does not seem to follow this trend. Dissolution efficiencies of the two systems at pH 10 at 60 min are 23.38% for bubble column and 29.76% for packed column (both at top of the column) (Table 4.1.1). Similarly, at 15th min, 45.28% for bubble column (Table 4.1.1) and 51.81% for packed column (both at top of the column) were observed. Obviously, the packed column could not deliver the enhanced mass transfer as expected (from

the high contacting area). Due to the path blockage in packed column, bubble was allowed to move more slowly. It resulted in slower slip velocity expressed as a smaller k (mass transfer coefficient) in following equation:

$$Sh = \alpha Re^\beta Sc^\gamma \quad (4.4)$$

where Sh = Sherwood number

Re = Reynolds number

Sc = Schmidt number

Equation (4.4) can be formulated to

$$\frac{kd}{D} = \alpha \left(\frac{\rho v D}{\mu} \right)^\beta \left(\frac{\mu}{\rho D} \right)^\gamma \quad (4.5)$$

where k = Mass transfer coefficient ($m \cdot min^{-1}$)

d = Diameter of column (m)

D = Mass diffusivity ($m^2 \cdot min^{-1}$)

ρ = Fluid density ($kg \cdot m^{-3}$)

v = Slip velocity or mean velocity ($m \cdot min^{-1}$)

μ = dynamic viscosity ($kg \cdot (m \cdot min)^{-1}$)

α, β and γ = constant number

Equation 4.5 suggests that slower slip velocity (v) could cause lower mass transfer coefficient resulting in a decrease in mass transfer rate (N). Fortunately, mass transfer area between gas

bubble and liquid (A) was enhanced by packing material. The influence of gas holdup and bubble diameter could be realized from the following analyses.

$$A = 4\pi \left(\frac{d_b^2}{2} \right) N_B \quad (4.6)$$

where

d_B = Bubble diameter (m)

N_B = Number of bubbles

ϵ_g is obtained from Equation 4.3, and can be re-written in terms of V_g as follows:

$$\epsilon_g = \frac{N_B \frac{4}{3} \pi \left(\frac{d_B}{2} \right)^3}{V_g} \quad (4.7)$$

Substitute N_B from Equation 4.7 to 4.6:

$$A = \frac{3\pi\epsilon_g V_g}{2d_B} \quad (4.8)$$

From Equation 4.8, an increase in gas hold up (ϵ_g) would give the better mass transfer rate (N) due to the higher A. However, packing material could cause bubble coalescence resulting in a larger bubble diameter (d_B) which decreased the mass transfer area proportionally. As a result, a twice increase in gas hold up did not enhance the %CO₂ dissolution efficiency as expected. Thus, adding packing material for improving gas-liquid contact area would only result in a slightly better in %CO₂ dissolution efficiency.

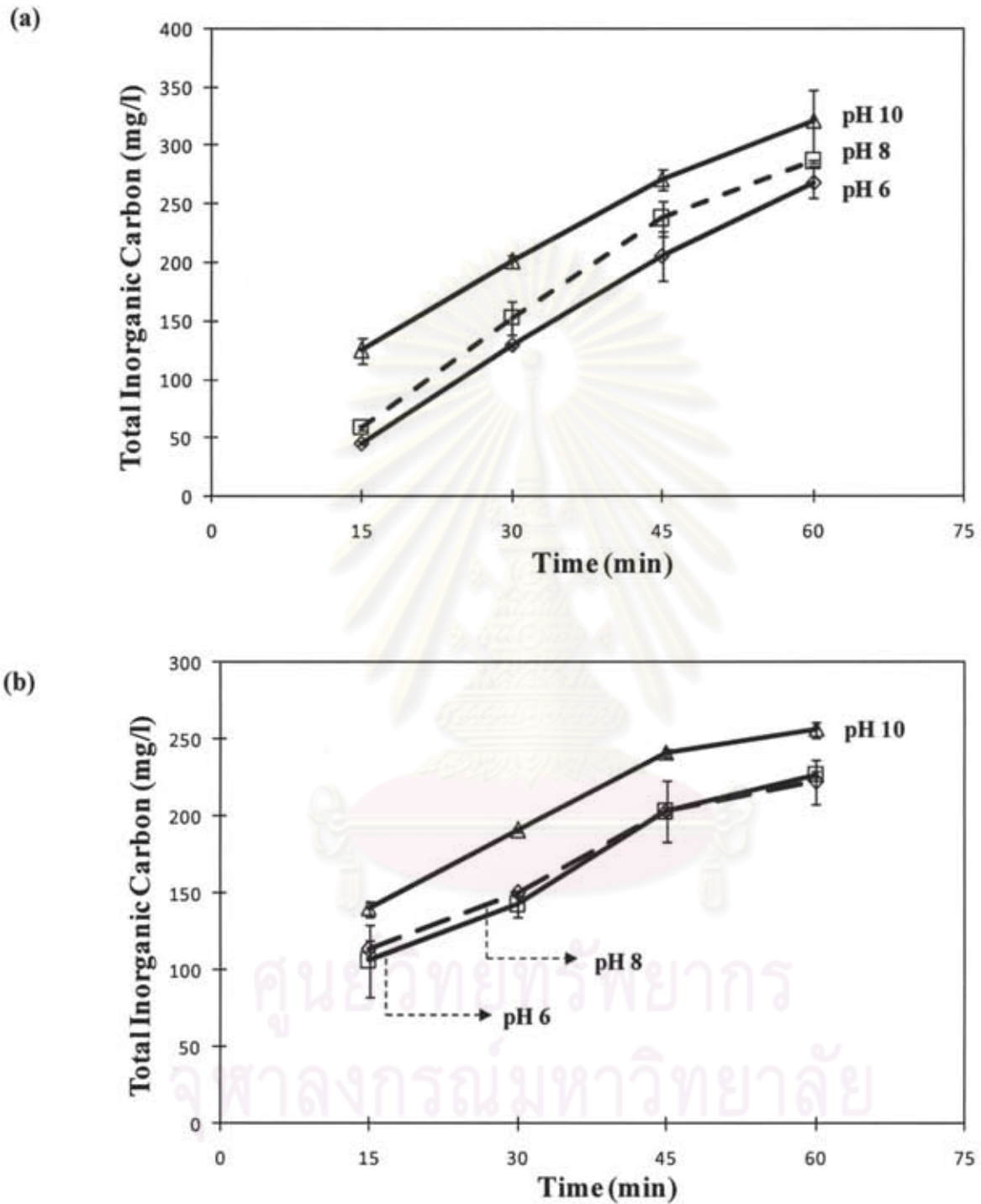


Figure 4.1.2.1 Total Inorganic Carbon time profile at various pH levels in bubble column with packing material (a) at top of the column (b) at middle of the column

Table 4.1.2 % Efficiency of CO₂ dissolution in packed column at various pH levels and positions

Time (min)	%Efficiency (Carbon Balance)					
	pH 6		pH 8		pH10	
	Top	Mid	Top	Mid	Top	Mid
15	16.83	21.77	42.00	39.33	46.15	51.87
30	23.93	28.22	27.80	26.47	37.21	35.33
45	25.37	29.32	25.11	25.05	33.41	29.83
60	24.84	26.53	20.58	21.04	29.76	23.74

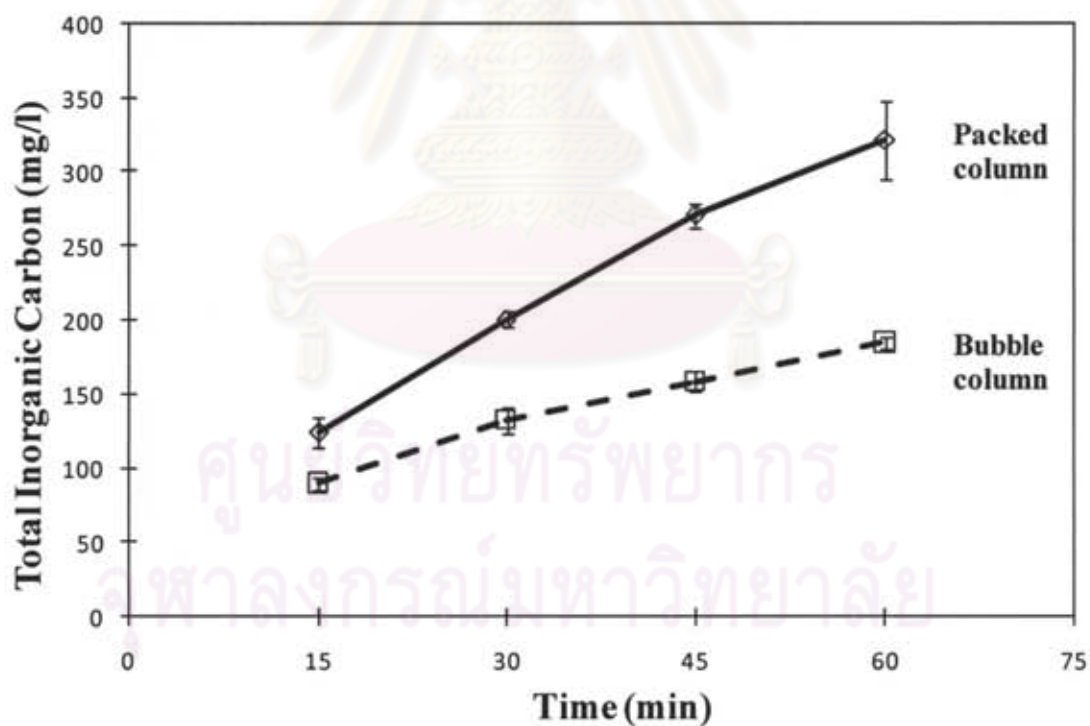


Figure 4.1.2.2 Total Inorganic Carbon time profile at pH 10 level in different column

4.1.3 Effect of gas-liquid contacting area on total inorganic carbon at pH 10 in 3 m high packed column

In this section, the fully packed column height was further upscaled from 1 m to 3 m to study the effect of height on CO₂ dissolution. TIC samples were collected and analysed at every 1m height interval and the associate %Efficiencies were calculated. Note that the experiments were operated at pH 10. The resulting TIC time profile is illustrated in Figure 4.1.3 where TIC increased with time and accumulated in the packed column. Because of inadequate contacting time at the beginning of the experiment, the 15th min TIC at different heights were not significantly different from each other. The 30th min TIC at 1 m height increased substantially and made the highest TIC concentration than at any other positions which could have resulted from the high concentration difference driving force at early stage as discussed earlier. At higher positions and later time period, the dissolved CO₂ (C₁) became high, lowering the concentration difference (ΔC) and so the mass transfer rate. However, CO₂ at 2 and 3m positions after 30 min was able to dissolve more steadily than at 1 m position as C₁ only increased gradually with time leading to a larger ΔC at the beginning, resulting in a steeper slope. Additionally, packed column allowed CO₂ to dissolve more effectively. As a large quantity of CO₂ was dissolved at the lower position, a lesser CO₂ was present at the top position. Therefore a lower TIC was also observed at the top position as a result. It should be noted that an increase in the column height may exhibit some influential factor to the mass transfer as the absolute pressure at 1 m location in the 3 metre column will be about 20% higher than the pressure at 1 m location in the 1 m or 2 m contactors. Increasing the pressure might have considerable effect to the bubble size and mass transfer rate and this was reflected in the higher initial mass transfer of CO₂ from gas to liquid.

%CO₂ dissolution efficiencies at different heights were computed and shown in Table 4.1.3. Clearly, efficiency at 1 m height was better than at 2m and 3m. The highest %efficiency at 1 m height was obtained at 30 min. However, computed %efficiencies at 2 m and 3 m increased with time from 15 min and achieved the highest %efficiency at 45th min. There were not significant differences between %efficiency at 45th and 60th min for both at 2 m (26.95% and 23.47%) and 3 m (19.41% and 17.51%) heights. Furthermore, at 30th, 45th and 60th

min, around 23-26% efficiency at 2 m position and around 10-19% efficiency at 3 m position were achieved.

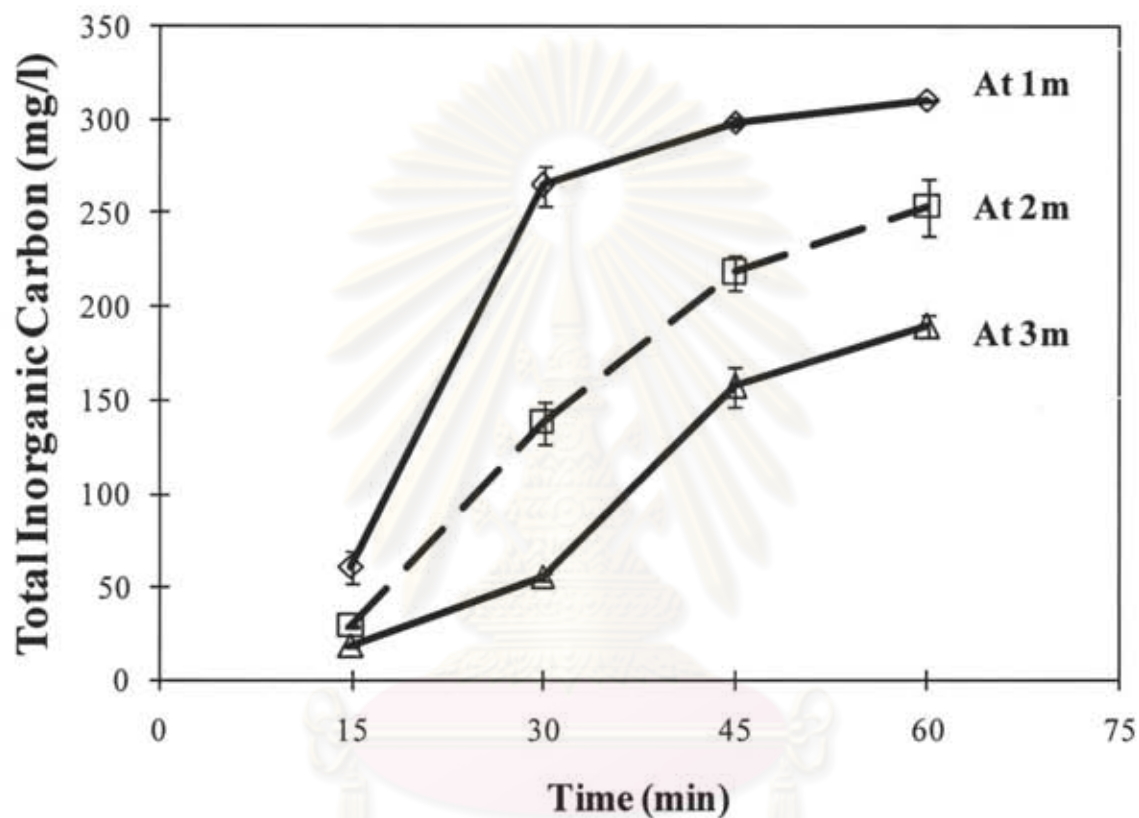


Figure 4.1.3 Total Inorganic Carbon time profile: samples collected various axial positions in the 3 meter high packed column

In summary, %efficiency was the lowest at the beginning and best at 30th min where the highest total % efficiency was obtained here at 78.39%. A triple increase in column height could result in better %efficiency but not triple times, e.g. 29.76% at 1 m high packed column (Table 4.1.2) and 64.35% at 3 m high packed column (at 60th min).

Table 4.1.3 % Efficiency of CO₂ dissolution in packed column at pH 10 and every 1 meter position

Time (min)	%Efficiency (Carbon Balance)			
	1m	2m	3m	Total
15	20.72	9.94	6.27	36.92
30	45.25	23.59	9.54	78.39
45	34.04	24.88	23.29	76.83
60	26.52	21.67	21.02	64.35

4.1.4 Effect of gas flowrate on CO₂ dissolution from 10-40 cc·min⁻¹ fed into the 1 and 2m high bubble column

Different CO₂ flowrates in range 10-40 cc·min⁻¹ were studied in this experiment to find out how gas flowrate affect CO₂ dissolution in the water. The experiment was conducted in 1 and 2 m high bubble columns at pH 10. For the 1 m high bubble column, the samples were collected at the top part of the column whereas, for the 2 m high bubble column, samples were collected at every 1 m height interval and the TIC time profiles at different gas flowrates were constructed as shown in Fig 4.1.4.1 along with the associated %CO₂ efficiencies in Table 4.1.4.1. Dissolved TIC increased and accumulated with time and the gas flow rate of 40 cc·min⁻¹ was shown to give the highest TIC level, whilst 10 cc/min exhibited the lowest trend. Besides, the average highest TIC concentration from 40 cc/min gas flowrate was achieved at 218.34 mg·L⁻¹ at 60th min. Increasing gas flowrate resulted in a higher TIC concentration trend over time.

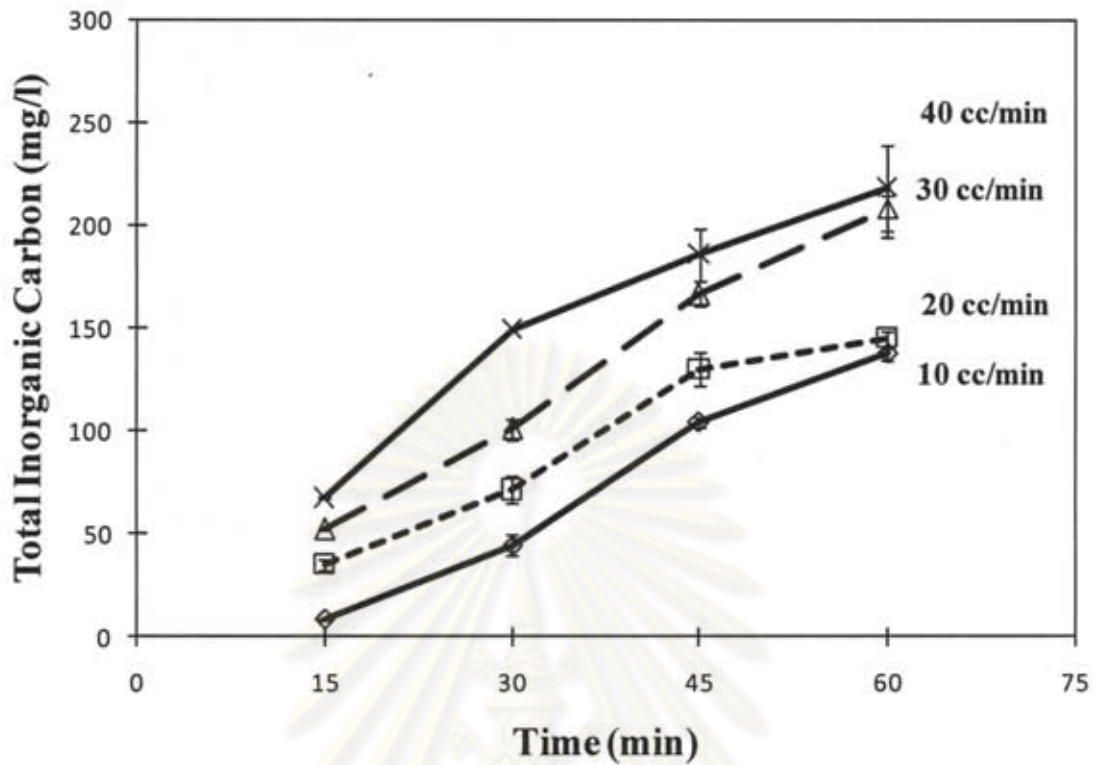


Figure 4.1.4.1 Total Inorganic Carbon at different time in 1 m bubble column: Effect of gas flowrate from 10-40 cc·min⁻¹

However, the calculated %efficiencies in CO₂ dissolution in Table 4.1.4.1 might not suggest an increase of flowrate. %CO₂ efficiency was high in the early stage of experiment and decrease with time for 10 cc·min⁻¹. This effect was not as clear when the flow rate increased to 20-40 cc·min⁻¹, e.g. for 40 cc·min⁻¹, %efficiencies varied in the range of 7.04-8.66. Distinctly, greater gas flowrate exhibited lesser %efficiencies with time and the undissolved gas would be released wastefully. Because of high slip velocity, an increase in gas flowrate was resulted in high mass transfer coefficient and rate. However, this reduced ΔC and made the system equilibrium more rapidly causing a decrease in %efficiency. On the contrary, greater amount of gas per time was could cause the higher C_1 appeared in bubble column and higher dissolved TIC concentration.

Table 4.1.4.1 % Efficiency of CO₂ dissolution in 1 m high column

Time (min)	%Efficiency (Carbon Balance)			
	10 cc·min ⁻¹	20 cc·min ⁻¹	30 cc·min ⁻¹	40 cc·min ⁻¹
15	30.94	10.64	7.47	8.66
30	29.98	14.71	9.53	7.45
45	23.86	12.27	9.40	7.04
60	21.11	11.02	8.91	7.64

In case of 2 m high bubble column, TIC time profiles at 1 m and 2 m height are shown in Figure 4.1.4.2(a) and 4.1.4.2(b), respectively. Dissolved TIC increased gradually and gathered with the time in the column. At 1 m position, at the beginning of experiment, it was no significant difference in dissolved TIC during the first 45 min as displayed in Figure 4.1.4.1(a). Similar to previous experiment in 1 m high column, an increase in gas flowrate would result in greater TIC dissolved in the water. The average highest TIC concentration was achieved at 60th min at 40 cc·min⁻¹ was 264.14 mg·L⁻¹. TIC concentration measured at 1 m high position in the 2 m column was in a similar range with that at the top of the 1 m column regardless of the flowrate employed. Nevertheless, an increase in the gas flowrate could be wastefully released as %efficiency of CO₂ dropped as shown in Table 4.1.4.2(a). In other words, the 10 cc/min gas flowrate provided the most efficient flowrate than any other flowrate where 30.94% efficiency was the highest obtained at 15th min.

Figure 4.1.4.2(b) represents TIC time profile at 2 m or at the top position where samples were collected. TIC trend at the top of the column (2 m) behaved slightly different from that at the middle of the column (1 m) (in Figure 4.1.4.2(a)). To begin with, in the first 30 min, the TIC concentrations at the top and middle parts were close at all flowrates. The deviation started to be well observed after 30 min where the 40 cc/min TIC provided the highest average TIC concentration of 250.10 mg·L⁻¹ at 60th min. The increase in TIC at higher gas flowrate could be due to the accelerating bubble velocity which facilitated the gas-liquid mass

transfer (as long as the system behaves in the bubbly flow regime). In contrast, the gas flowrate of $10 \text{ cc}\cdot\text{min}^{-1}$ gave the lowest level of dissolved TIC. Despite so, %Efficiencies of CO_2 dissolution was found to be the highest at $10 \text{ cc}\cdot\text{min}^{-1}$ as most of CO_2 in the inlet gas stream could dissolve into the water (Figure 4.1.4(b)). On the other hand, a greater quantity of CO_2 did not have enough contact time with the solution and was wastefully released to the atmosphere.

In addition, bubble column always exhibited the plug flow – like behaviour at low gas throughput. This behaviour gradually changed to the well mixed as the gas flowrate increased. As a result, greater gas flowrate led to the accumulation of dissolved TIC at the top of the column due to higher velocity and greater bubble diameter. Figure 4.1.4(a) and 4.1.4(b) depicts that there were large differences between the axial TIC concentrations (i.e. at 1 m and 2 m height) particularly at low gas flowrates (10 and $20 \text{ cc}\cdot\text{min}^{-1}$), and the differences seemed to be insignificant at higher gas flowrates ($40 \text{ cc}\cdot\text{min}^{-1}$). This could be due to the different mixing behaviour as the higher flowrate seemed to be able to induce more back-mixing and the behaviour of the system became closer to the completely mixed pattern. On the other hand, the column behaved closer to a plug flow mode at low gas flowrate.

In summary, an increase in gas flow rate might enhance the CO_2 solubility, but at this condition, most of the CO_2 was just released to the atmosphere, resulting in the low %efficiency in CO_2 dissolution. Hence, it might not be worthwhile to feed the gas at high flowrate into the bubble column. Besides, an increase in height without adding gas contacting area could not effectively provide a satisfactory level of efficiency in CO_2 dissolution (when compared with the shorter column).

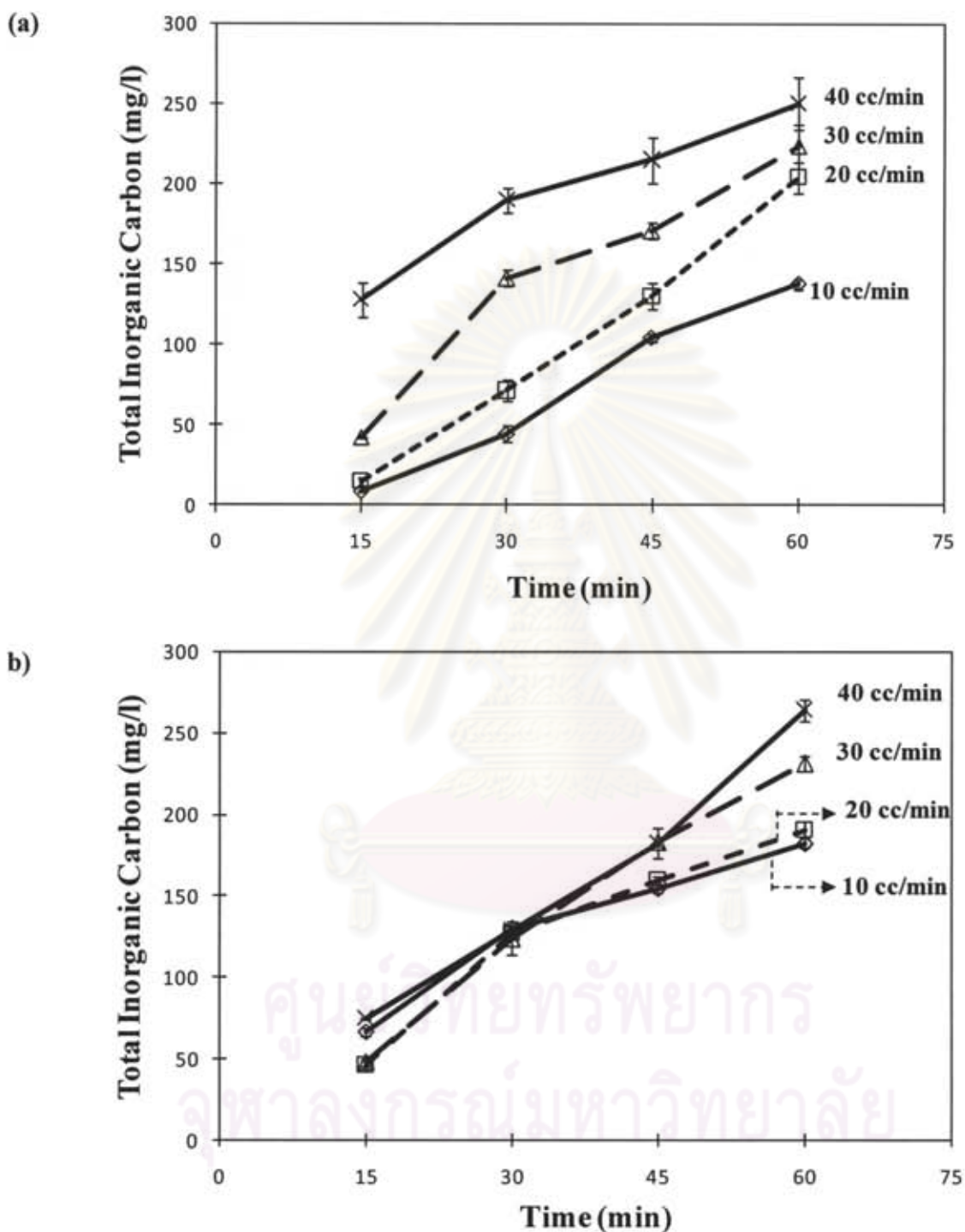


Figure 4.1.4.2 Total Inorganic Carbon at different time: effect of gas flowrate from 10-40 cc·min⁻¹ on Total Inorganic Carbon concentration and samples collected (a) at 1m height (b) at 2m height

Table 4.1.4.2 (a) % Efficiency of CO₂ dissolution in 2 m high column: samples collected at 1 m position

Time (min)	%Efficiency			
	10 cc/min	20 cc/min	30 cc/min	40 cc/min
15	30.94	10.64	7.47	8.66
30	29.98	14.71	9.53	7.45
45	23.86	12.27	9.40	7.04
60	21.11	11.02	8.91	7.64

Table 4.1.4.2 (b) % Efficiency of CO₂ dissolution in 2 m high column: samples collected at 2 m position

Time (min)	%Efficiency			
	10 cc·min ⁻¹	20 cc·min ⁻¹	30 cc·min ⁻¹	40 cc·min ⁻¹
15	4.08	3.44	6.49	14.79
30	10.31	8.27	10.88	11.00
45	16.09	10.05	8.79	8.29
60	15.95	11.81	10.34	7.23

ศูนย์วิทยทรัพยากร
จุฬาลงกรณ์มหาวิทยาลัย

4.1.5 Effect of salinity on CO₂ dissolution

CO₂ dissolution in the salt water has great application as many microalgae are marine species and their growth would require the carbon source in some particular forms. Various salinity levels from 0 to 30 ppt (part per thousand) were carried out in this experiment. The pH value of the fresh control experiment was set at pH 8 which was the closest to that of the brine solution. An experiment was taken place in the 1 m high bubble column. Dissolved TIC was increased with time and was accumulated in the bubble column. The presence of salinity lowered the dissolution of TIC in the solution. Clearly, the highest salinity in this experiment, 30 ppt, resulted in lowest TIC trend than others. For fresh (0 ppt) and brackish water (5 ppt), TIC was not quite distinctly different at the beginning but the difference became clearer at the later stage of the experiment. %efficiency of CO₂ dissolution at various salinity levels is reported in Table 4.1.5. The highest %efficiency at every time sample collected was achieved at zero level of salinity (fresh water) whereas the highest salinity in this experiment, at 30 ppt, exhibited the lowest %efficiency than the others. Higher degree of salinity means water contains higher dissolved salt contents, e.g. sodium chloride, magnesium and calcium sulfate. These might lower the solubility, especially at higher degree of salinity. As the result, CO₂ solubility become lower than that observed in fresh water.

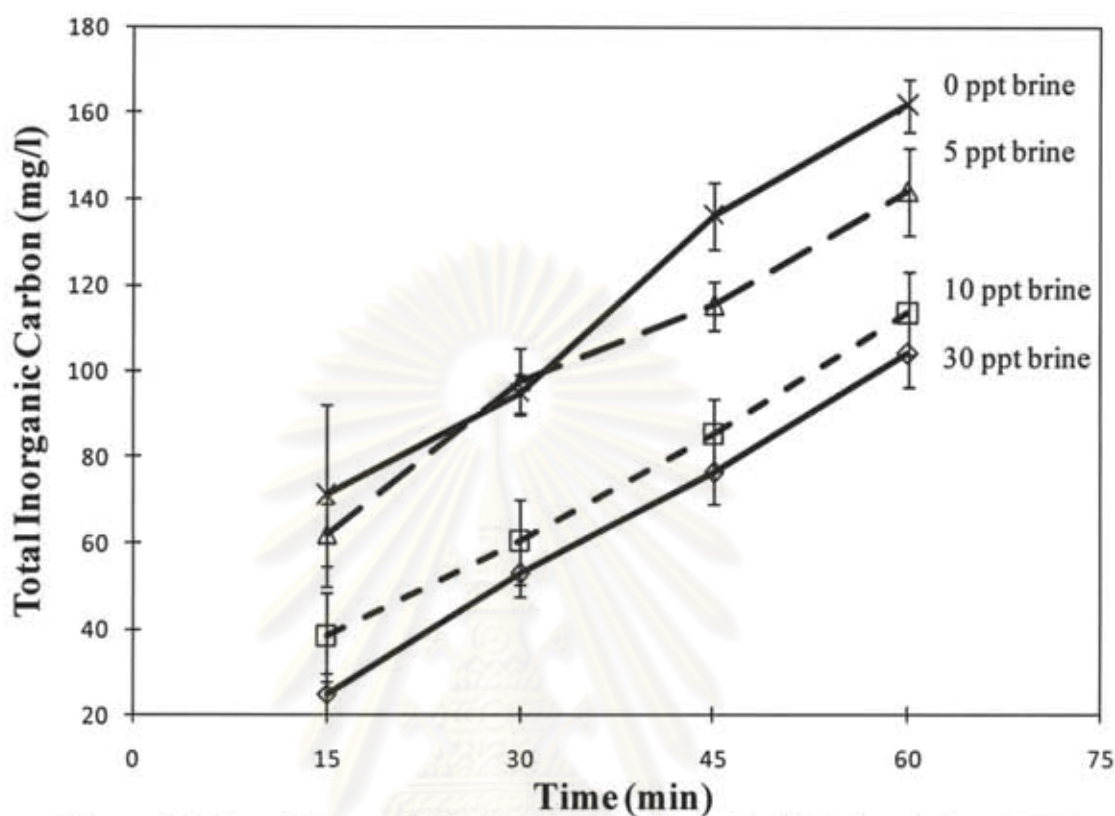


Figure 4.1.5 Total Inorganic Carbon time profile and salinity levels from 0-30 ppt

Table 4.1.5 %Efficiency of CO₂ dissolution at various salinity levels from 0-30 ppt

Time (min)	%Efficiency			
	0 ppt	5 ppt	10 ppt	30ppt
15	35.83	31.19	19.24	12.51
30	26.31	27.09	15.19	13.32
45	25.20	19.38	14.32	12.82
60	22.47	17.88	14.31	13.13

4.1.6 CO₂ dissolution using Circulating Counterflow Contactor (C.C.C.)

Previously, the effects of pH, liquid-gas contacting area, column height and gas flowrate were studied for their influence on the dissolution of CO₂ in the water. In this section, the optimal combined effects led to the new cooperated system design; it was thereafter called "Circulating Counterflow Contactor- C.C.C" 1 m packed column was implemented and the flow configuration was changed from static to recycle flow in which it allowed gas and water to contact in opposite direction in the reactor. The 5 litres reservoir was united in the flow system to allow a more effective recirculation of the water. The recirculating liquid flowrate was varied from 1 to 3 LPM (Litres per minute), gas flow rate was controlled at 10 cc/min and the pH at 10. Figure 4.1.6 demonstrates the TIC time profile at different recirculating flowrates whereas Table 4.1.6 reports the %efficiency of the system. TIC increased with time and accumulated in the column, and the recirculating flowrate that gave the highest TIC concentration was 2 LPM. The highest %efficiency was achieved at 56.01% at the first 15 minutes but this seemed to slightly decrease with time.

The better CO₂ dissolution with C.C.C. system was resulted from two particular reasons; (1) an increase in slip velocity due to the recycle flowrate of liquid and (2) the diminishing concentration difference (ΔC) barrier. Firstly, applying of recirculating flowrate of liquid from the top of the column in the transverse direction with gas resulted in gas bubble being in contact with liquid at a longer time period, allowing gas to dissolve in liquid more. Additionally, gas bubbles did not show coalescing behaviour in such dynamic condition when compared with that in the static condition. This resulted in a smaller bubble, or higher mass transfer area which consequently provided a higher mass transfer rate. For the second reason, larger ΔC was found in this system as the more well mixed condition lowered the average C_1 leading to a greater concentration different driving force. Thus, high % CO₂ dissolution efficiencies could be found not only the early stage but also at the later stage.

From these reasons above, C.C.C. might be the successful combined effect for CO₂ dissolution system in which the most optimal recycle flowrate was employed at 2 LPM. Next, utilize captured CO₂ for microalgal cultivation purpose will be studied in section 4.2.

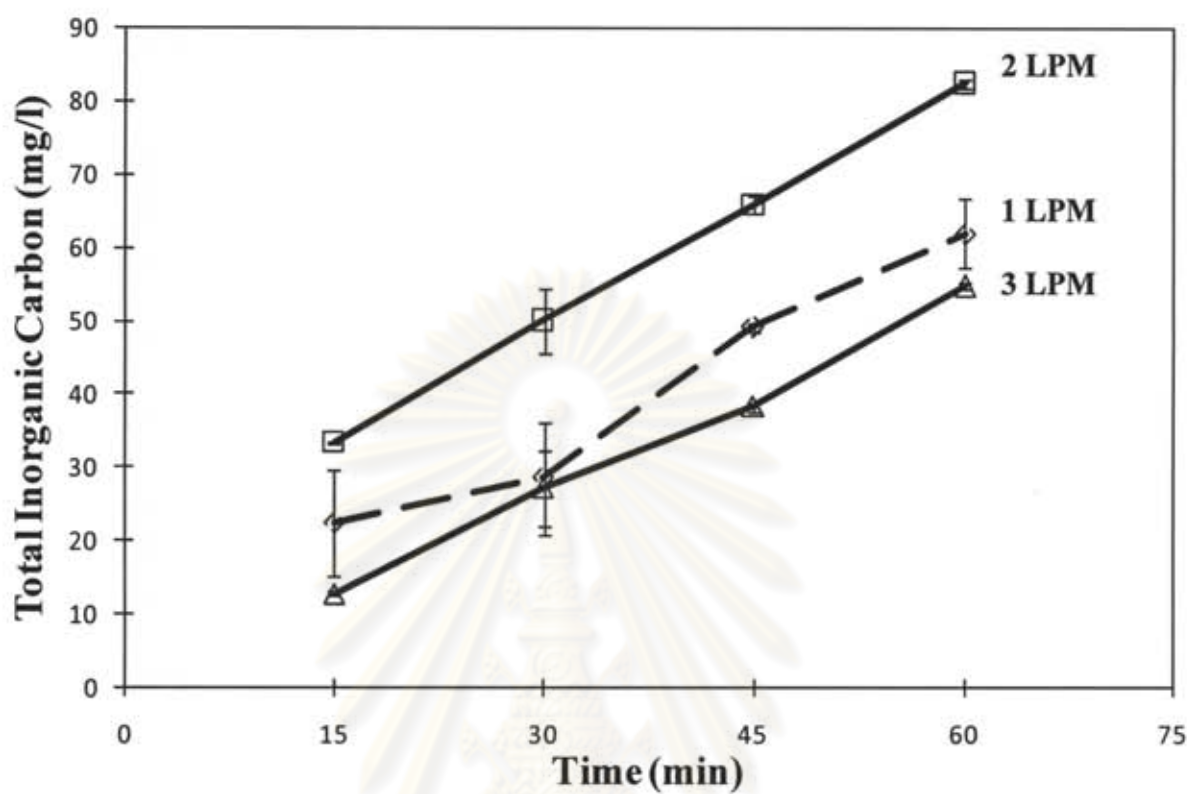


Figure 4.1.6 Total Inorganic Carbon at different time at various recirculating flows in the gas-liquid contacting bubble column, using recycle flow in a range of 1-3 LPM (Litres per minute)

Table 4.1.6 %Efficiency of CO₂ dissolution using recycle flow of 1-3 LPM

Time (min)	%Efficiency		
	1 LPM	2 LPM	3 LPM
15	37.56	56.01	21.40
30	23.92	42.05	22.80
45	27.54	36.90	21.47
60	26.06	34.70	23.02

4.2 Accelerating microalgal growth with bicarbonate as inorganic carbon source

4.2.1 Cultivation of *C. vulgaris* with NaHCO_3 at various pH range

The cultivation of *Chlorella vulgaris* was investigated in various range of pH cultivating condition. Originally, modified M4N (Morita et al., 2000) is reported to be suitable for the growth of *Chlorella vulgaris*, and this medium, without the addition of NaHCO_3 , was employed as a blank experiment. Note that this medium is without the presence of NaHCO_3 and the carbon source is the CO_2 from aeration. Unlike CO_2 , bicarbonate ion (HCO_3^-) can be dissolved well in the water due to its high solubility and it is the aim of this work to investigate whether this readily soluble form of carbon (bicarbonate) benefit the growth of such alga. Importantly, using bicarbonate compound for microalgal cultivation requires that the pH of the solution be initially adjusted to a proper range, and it was examined in this section how the pH could affect the growth of the alga. To achieve this, NaHCO_3 at 30 ppm was added to the medium at various initial pH (from 6 to 9). Cell concentration time profile illustrated in the Figure 4.2.1 displayed the experimental results. It took approximately 6 days for the cell to reach its stationary phase where the averaged maximum cell concentration achieved from pH 6, 7, 8 and 9 conditions were 106, 105, 73.75 and 42.13 million cells per millilitre, respectively. pH around 6 and 7 seemed to give the best cell growth above which the growth started to drop, and it was obvious that pH 9 was, by all means, not suitable for cell growth (as some of the bicarbonate can be transformed to carbonate which could not be uptaken by the cell). It is interesting that the cultivation at pH 8 gave a better result than the blank test in which the initial pH was around 7.2. The growth rate can be calculated from the log phase period as the specific growth rate (μ) in unit h^{-1} and d^{-1} and shown in Table 4.2.1. The highest specific growth rate was acquired at 0.045 h^{-1} or 1.080 d^{-1} at pH 7. 0.043 h^{-1} or 1.032 d^{-1} at pH 6, 0.040 h^{-1} or 0.960 d^{-1} at pH 8 and 0.034 h^{-1} or 0.816 d^{-1} at pH 9.

Distinctly, enhancing microalgal growth with bicarbonate as inorganic carbon for microalgal cultivation offered the higher maximum cell concentration and specific growth rate compared with the case without bicarbonate (blank test). From the finding, suitable initial

pH value for *C. vulgaris* cultivation was in the range of 6-7 in which utilization of bicarbonate was most effective.

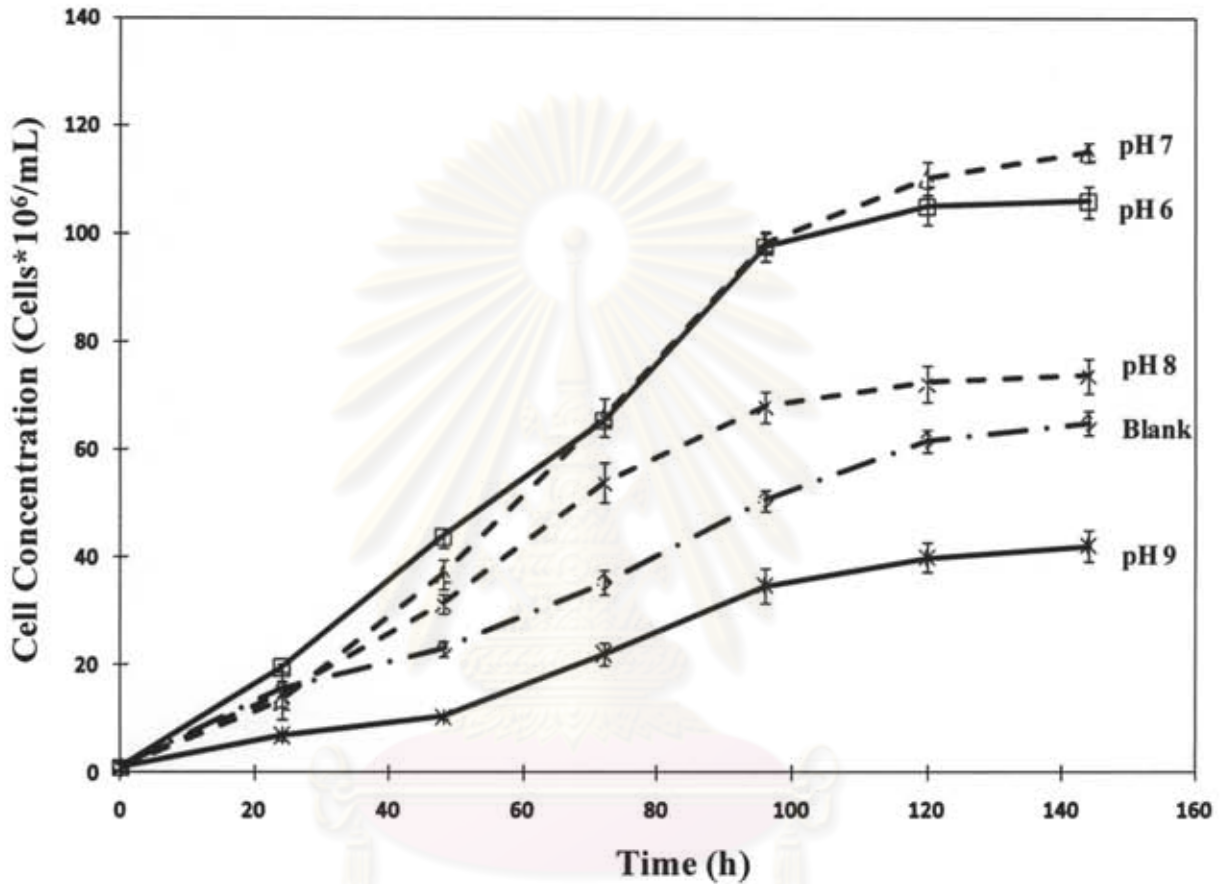


Figure 4.2.1 Growth curve of *Chlorella vulgaris* cultivation with 30 ppm NaHCO_3 as inorganic carbon at various pH ranges from 6-9

จุฬาลงกรณ์มหาวิทยาลัย

Table 4.2.1 Maximum cell concentration and specific growth rate (μ) of *Chlorella vulgaris* cultivation with 30 ppm NaHCO_3 as inorganic carbon source at various initial pH conditions

Condition	Maximum cell conc. (cells* 10^6 ml $^{-1}$)	μ (h $^{-1}$)	μ (d $^{-1}$)
Blank	65	0.036	0.864
pH 6	106	0.043	1.032
pH 7	115	0.045	1.080
pH 8	74	0.040	0.960
pH 9	42	0.034	0.816

4.2.2 Cultivation of *C. vulgaris* with high concentration of NaHCO_3 and CO_2 dissolved water form C.C.C. as inorganic carbon at pH 7

In this section, initial adjusted medium at pH 7 was employed with higher concentration of NaHCO_3 , i.e. from 30 to 200 $\text{mg}\cdot\text{L}^{-1}$ (ppm) to investigate its effect on microalgal growth. In addition, the pH-adjusted CO_2 dissolution water from the C.C.C. system in Section 4.1.5 (at 2 LPM) was also employed to cultivate the alga. It is noted that this solution contained approximately 80 ppm of TIC. Besides, the cultivation with equivalent concentration of NaHCO_3 at 80 ppm was also conducted to compare the result with the medium with CO_2 dissolution water. Cell concentration time profile with different amounts of bicarbonate is shown in Figure 4.2.2.

จุฬาลงกรณ์มหาวิทยาลัย

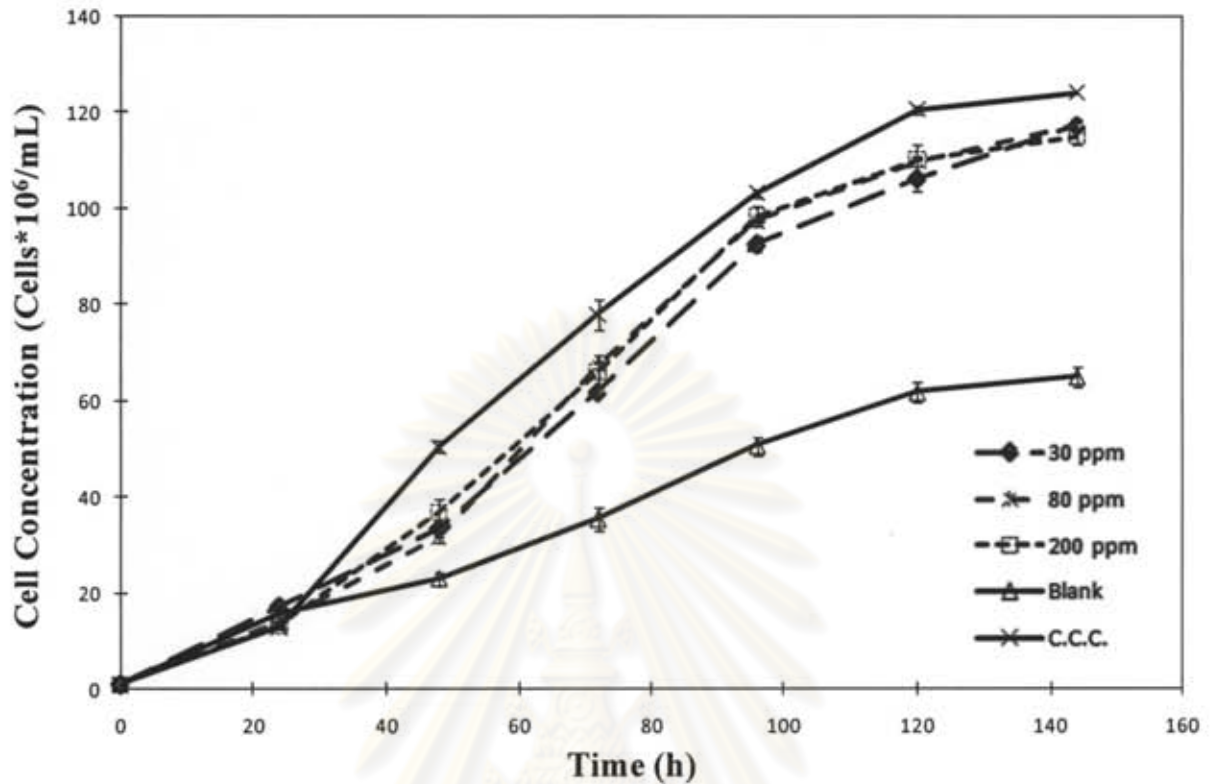


Figure 4.2.2 Growth curve of *C. vulgaris* cultivated with various 0, 30, 80 and 200 ppm NaHCO_3 and water from CO_2 dissolved water from C.C.C. as inorganic carbon at initial pH 7 condition

Obviously, the cultivation in blank medium (without NaHCO_3) was the lowest which illustrates well that this microalga could uptake the carbon in bicarbonate form. However, not significantly different growth curves were clearly observed from the cultivation with 30, 80 and 200 ppm NaHCO_3 where the maximum cell concentrations at the various conditions are reported in Table 4.2.2. Only a slight difference in specific growth rate was obtained; 1.080, 1.056 and 1.032 d^{-1} for the cultivation at 30, 80 and 200 ppm NaHCO_3 , respectively. However, CO_2 dissolution water from the C.C.C system (at 2 LPM) displayed the greater trend in cell concentration time profile compared with other cultivation with the addition of NaHCO_3 where the maximum cell concentration and specific growth rate were obtained at 124 million cells per millilitre and 1.104 d^{-1} , respectively. This verifies that *Chlorella vulgaris* could be well cultivated using carbon source from the solution obtained from the CO_2 absorption column. When

compared the results with the medium with 80 ppm NaHCO_3 , the growth in the C.C.C. water seemed to give a slightly better result, which could be due to the error from experiment.

Table 4.2.2 Maximum cell concentration and specific growth rate (μ) of *Chlrollera vulgaris* cultivation with various amount of NaHCO_3 as inorganic carbon source at initial pH 7 condition

Condition	Maximum cell conc. (cells* 10^6 ml $^{-1}$)	μ (h $^{-1}$)	μ (d $^{-1}$)
Blank	65	0.036	0.864
30ppm NaHCO_3	115	0.045	1.080
80ppm NaHCO_3	117	0.044	1.056
200ppm NaHCO_3	118	0.043	1.032
C.C.C. water	124	0.046	1.104

ศูนย์วิทยทรัพยากร
จุฬาลงกรณ์มหาวิทยาลัย

CHAPTER V

CONCLUSIONS AND RECOMMENDATIONS

5.1 Conclusions

The investigation in this work led to the following conclusions:

1. An increase in pH could lead to a greater dissolution of CO₂ resulting in a greater TIC concentration trend and %CO₂ dissolution efficiency.
2. High %efficiency was found in the early stage of experiment and later was decreased with time due to the concentration difference between gas phase and liquid phase.
3. Adding gas-liquid contact area and gas hold up (ϵ_g) caused a slightly greater dissolution of CO₂ due to the slower slip velocity by path blockage and bubble was coalescence resulting in large bubble diameter of gas and decreased mass transfer rate.
4. A triple increase in height in packed column gave the better overall %efficiency but not in direct proportional in triple times. Furthermore, concentration in gas decreased along the axial position resulting in low TIC concentration in higher position.
5. A greater gas flowrate fed into the system displayed a higher TIC concentration due to an accelerating bubble velocity which enhanced the gas-liquid mass transfer. However, a greater quantity of CO₂ did not have enough contact time with the solution and wastefully released to the atmosphere causing low %efficiency.

6. Higher degree of salinity gave the lower TIC dissolved in the water. Fresh water exhibited the higher TIC trend and %efficiency at any time than salt water.
7. The optimal combined effects from previous findings led to the system design of better CO₂ dissolution called "Circulating Counterflow Contactor- C.C.C". It allowed liquid and gas to contact in transverse direction. This would provide the longer dissolution period and gas bubbles did not show coalescing behaviour in this system. As a result, C.C.C. offered the steadily high %efficiency not only in early stage but also later stage in range 34-56% in the case where 2 LPM optimal flowrate was employed.
8. The most suitable initial pH for cultivating fresh water microalgae *Chlorella vulgaris* with NaHCO₃ were 6 and 7 in which maximum cell concentration and specific growth rate were slightly different. On the contrary, pH 8 and 9 did not suit the *C. vulgaris* cultivation.
9. An increase in NaHCO₃ concentration in the cultivation system from 30 to 80 and 200 ppm did not particularly give the different in growth characteristic. Besides, CO₂ dissolution water from C.C.C. (around 80 ppm TIC concentration) provided a slightly higher in growth curve, maximum cell concentration and specific growth rate. This proved that CO₂ dissolved water from CO₂ dissolution system could be implemented for the microalgal cultivation.

5.2 Contributions

To mitigate greenhouse effect, many CO₂ capture and storage technologies are employed in a wide range of industries. Sequestration of CO₂ into a biomass form is considered to be the potentially sustainable method. Microalgae have the capability of conducting highly effective photosynthetic activity in which CO₂ is turned into the form of microalgal biomass but this transformation rate is much too low when compared with the rate at which CO₂ is being released to the atmosphere. This work introduces the transformation of CO₂ into the other forms, e.g. bicarbonate and carbonate compounds which could later be used as carbon source for the

microalgae. This system will act like a buffer zone where CO₂ is being captured prior to feeding to the algal culture. CO₂ dissolution water was proved in accelerating *C. vulgaris* growth (compared with the no addition of inorganic carbon). These preliminary results provide an encouraging indication to the future development of CO₂ capturing technology where the two step approach could be treated as a potential direction.

5.3 Recommendations / Future works

This work only presents the beginning of CO₂ sequestration by capturing CO₂ and prior storage for the microalgal uptake instead of feeding CO₂ directly into the cultivation system. Many fundamental effects were studied in this work e.g. pH, gas-liquid contact, salinity and column height. Moreover, the captured CO₂ in the liquid form was proved to be applicable as a carbon source for the cultivation of microalgae *C. vulgaris*. The next step towards the implementation of such technology is to upscale the CO₂ dissolution system as a pilot study along with the actual size microalgal cultivating system. The use of actual CO₂ from the flue gas should also be investigated.

ศูนย์วิทยทรัพยากร
จุฬาลงกรณ์มหาวิทยาลัย

REFERENCES

- Anabades, J. C., Anthony E. J., Alvarez D., Lu, D.Y., and Salvador, C. (2004a). Capture of CO₂ from Combustion Gases in a Fluidised Bed of CaO. AIChE Journal 50(7): 1614-1622.
- Anabades, J. C., Rubin E. S., and Anthony E. J. (2004b). Sorbent cost and performance in CO₂ capture systems. Industrial and Engineering Chemistry Research 43: 3462-3466.
- Bai, H., and Yeh, A. C. (1997). Removal of CO₂ Greenhouse Gas by Ammonia Scrubbing. Industrial & Engineering Chemistry Research 36(6): 2490-2493.
- Berman-Frank, I., Erez, J. and Kaplan, A. (1998). Changes in inorganic carbon uptake during progression of a dinoflagellate bloom in a lake ecosystem. Journal of Botany 76: 1043-1051.
- Bonenfant, D., Mimeault, M., and Hausler, R. (2003). Determination of the structural features of distinct amines important for the absorption of CO₂ and regeneration in aqueous solution. Industrial and Engineering Chemistry Research 42(14): 3179-3184.
- Bozzo, G. G., Colman, B. et al. (2000). Active transport of CO₂ and bicarbonate is induced in response to external CO₂ concentration in the green alga *Chlorella kessleri*. Journal of Experimental Botany 51(349): 1341-1348.
- Brewer, P. G., Glover, D. M., Goyet, C. and Shafer, D .K. (1995). The pH of the North Atlantic Ocean: improvements to the global model for sound absorption in seawater. J. Geophys. Res , 100: 8761–8776.
- Burkhardt, S., Amoroso, G., Riebesell, U., and Sultemeyer D. (2001). CO₂ and HCO₃⁻ uptake in diatoms acclimated to different CO₂ concentrations. Limnol Oceanogr 46: 1378-1391.
- Chen, H., Kovvali, A. S., Majumdar, S., and Sirkar, K. K. (1999). Selective CO₂ separation from CO₂-N₂ mixtures by immobilised carbonate-glycerol membranes. Industrial and Engineering Chemistry Research 38: 3489-3498.
- Fleischer, C., Becker, S. and Eigenberger, G. (1996). Detailed modeling of the chemisorption of CO₂ into NaOH in a bubble column. Chemical Engineering Science, 51(10): 1715-1724
- Coleman, B. and Rotalore C. (1995). Photosynthetic inorganic carbon uptake and accumulation in two marine diatoms. Plant, Cell and Environment 18(8): 919-924.

- Colman, B., Huertas, I. E., Bhatti, S., and Dason, J. S. (2002). The diversity of inorganic carbon acquisition mechanisms in eukaryotic microalgae. Functional Plant Biology 29: 261-270.
- Coninck, B. M., and Meyer, M. L. L. (2005). Carbon Dioxide Capture and Storage. New York, USA, Cambridge University Press.
- Continex (2009). Chlorella. [Online]. Available from : <http://www.continex.com/chlorella.htm>. [2010, May 1]
- Dason, J. S., Huertas I. E., and Colman, B. (2004). Source of Inorganic Carbon For Photosynthesis in Two Marine Dinoflagellates. Phycological Society of America 40(285-292).
- David R. L. (1991). CRC Handbook of Chemistry and Physics, 71 ed. Boca Raton, Ann Arbor, Boston: CRC Press.
- de Morais, M. G. and Costa J. A. V. (2007). Biofixation of carbon dioxide by *Spirulina* sp. and *Scenedesmus obliquus* cultivated in a three-stage serial tubular photobioreactor. Journal of Biotechnology 129(3): 439-445.
- Dong, L. F., Nimer, N. A., et al. (1993). Dissolved inorganic carbon utilization in relation to calcite production in *Emiliana huxley* (Lohmann) Kamptner. New Phytologist 123(4): 679-684.
- Eva, L. D., and Reski, R. (2007). Moss bioreactors producing improved biopharmaceuticals. Current Opinion in Biotechnology 18: 393-398.
- Feron, P. H. (1994). Membranes for carbon dioxide recovery from power plants. Carbon dioxide Chemistry: Environmental issues Cambridge, UK, The Royal Society of Chemistry.
- Feron, P. H. (2002). CO₂ Separation with polyolefin membrane contactors and dedicated absorption liquids Performances and prospects. Separation and Purification Technology 27(3): 231-242.
- Goldberg, F. (2008). Rate of Increasing Concentrations of Atmospheric Carbon Dioxide Controlled by Natural Temperature Variations. Energy & Environment, 19(7): 995-1011
- Giordano, M., Beardall, J., et al. (2005). CO₂ CONCENTRATING MECHANISMS IN ALGAE: Mechanisms, Environmental Modulation, and Evolution. Annual Review of Plant Biology 56(1): 99-131.
- Green, D. A., et al. (2002). Capture of Carbon Dioxide from flue gas using regenerable sorbents. 19th Annual International Pittsburgh Coal Conference, Pittsburgh, Pennsylvania.

- Hendriks, C. (1994). Carbon dioxide removal from coal-fired power plants. Doctoral dissertation, Utrecht University, Netherlands.
- Herzog, H., Golomb, D., and Zemba, S. (1991). Feasibility, modeling and economics of sequestering power plant CO₂ capture emissions in the deep ocean. Environmental Progress 10(1): 64-74.
- Hoffman, J. S., Fauth, D. J., and Pennline, H. W. (2002). Development of novel dry regenerable sorbents for CO₂ capture. 19th Annual International Pittsburgh Coal Conference.
- Hsunling, B., and An Chin Yeh. (1999). Comparison of ammonia and monoethanolamine solvents to reduce CO₂ greenhouse gas emissions. The Science of the Total Environment 228: 121-133.
- Huertas, I. E., Colman, B., et al. (2000). Active transport of CO₂ by three species of marine microalgae. Journal of Phycology 36(2): 314-320.
- Huertas, I. E., Colman, B., et al. (2000a). Active transport of CO₂ by three species of marine microalgae. Journal of Phycology 36(2): 314-320.
- Huertas, I. E., Espie, G. S., et al. (2000b). Light-dependent bicarbonate uptake and CO₂ efflux in the marine microalga *Nannochloropsis gaditana*. Planta 211(1): 43-49.
- Huntley, M. E. (2007). CO₂ MITIGATION AND RENEWABLE OIL FROM PHOTOSYNTHETIC MICROBES: A NEW APPRAISAL. Mitigation and Adaptation Strategies for Global Change 12: 573-608.
- Ishibashi, M., Otake, K., Kanamori, S. and Yasuke, A. (1999). Study on CO₂ Removal Technology from flue gas of Thermal Power Plant by Physical Adsorption Method. Greenhouse Gas Control Technologies 95-100.
- James, T., Yeh, T., Resnik, K. P., Kathy, R., and Pennline, H.W. (2005). Semi-batch absorption and regeneration studies for CO₂ capture by aqueous ammonia. Fuel Processing Technology 86 1533- 1546.
- Je, Y. K., Kunwoo Han and Hee Dong Chun. (2009). CO₂ absorption with low concentration ammonia liquor. Energy Procedia 1: 757-762.
- Jou, F. M. and Otto, F. D. (1995). The Solubility of CO₂ in a Mass Percent Monoethanolamine Solution. Journal of Chemical Engineering 73: 140-147.
- Kaplan, A., Volokita M., Zenvirth, D. and Reinhold, L. (1984). An essential role for sodium in the bicarbonate transport system of the cyanobacterium *Anabaena variabilis*. FEBS Letters 176(166-168).

- Kim, Y. J., et al. (2008). Characteristics of CO₂ Absorption into Aqueous Ammonia. Separation Science and Technology 43(4): 766-777.
- Kohl, A. O. (1997). Gas Purification. Houston, TX, USA., Gulf Publisher Co., .
- Korb, R.E., Johnston, A.M., and Raven, J. A. (1997). Sources of inorganic carbon for photosynthesis by three species of marine diatom. Journal of Phycology 33: 433-440.
- Kovvali, A. (2001). Dendrimer liquid membranes separation from gas mixtures. Industrial and Engineering Chemistry Research 40(2502-2511).
- Kurano, N. (1995). Fixation and Utilization of Carbon Dioxide by Microalgal Photosynthesis. Energy Conversion Management 36(6-9): 689-692.
- Leggat, W., Badger, M. R. and Yellowlees D. (1999). Evidence for an inorganic carbon-concentrating mechanism in the symbiotic dinoflagellate *Symbiodinium sp.* Plant Physiology 121: 1247-1255.
- Li, Y., Horsman, M., Wu, N., Lan, C. Q., and Dubois-Calero, N. (2008). Biofuels from microalgae. Biotechnology Progress 24(4): 815-820.
- Lin, C. C., Liu, W. T., and Tan, C. S. (2003). Removal of carbon dioxide by absorption in a rotating packed bed. Industrial and Engineering Chemistry Research 42(11): 2381-2386.
- Maeda, K., Owada, M., Kimura, N., Omata, K., and Karube, I. (1995). CO₂ fixation from the flue gas on coal-fired thermal power plant by microalgae. Energy Conversion Management 36: 717-720.
- Matsumoto, H., Hamasaki, A., Sioji, N., and Ikuta, Y. (1997). Influence of CO₂, SO₂ and NO in flue gas on microalgae productivity. Japan Journal of Chemical Engineering 30: 620-624.
- Merrett, M. J., Nimer, N. A., et al. (1996). The utilization of bicarbonate ions by the marine microalga *Nannochloropsis oculata* (Droop) Hibberd. Plant, Cell and Environment 19(4): 478-484.
- Morel, F., et al. (2002). Acquisition of inorganic carbon by the marine diatom *Thalassiosira*. Functional Plant Biology 29: 301-308.
- Nakagawa, K., and Ohashi, T., (1998). A novel method of CO₂ capture from high temperature gases. Journal Electrochem Society, 145(4): 1344-1346.

- Nimer, N. A., Brownlee, C., and Merrett, M. J. (1999). Extracellular carbonic anhydrase facilitates carbon dioxide availability for photosynthesis in the marine dinoflagellate *Prorocentrum micans*. Plant Physiology 120: 105-111.
- Okabe, K., Matsumija, N., Mano, H., and Teramoto, M. (2003). Development of CO₂ separation membranes (1) Facilitated transport membrane. In Greenhouse Gas Control Technologies: 1555-1558.
- Pipitone, G. and Bolland, O. (2009). Power generation with CO₂ capture: Technology for CO₂ purification. International Journal of Greenhouse Gas Control 3(5): 528-534.
- Quinn, R., and Laciak, D.V. (1997). Polyelectrolyte membranes for acid gas separations. Journal of Membrane Science 131: 49-60.
- Reski, E. L. (2007). Moss bioreactors producing improved biopharmaceuticals. Current Opinion in Biotechnology 18: 393-398.
- Resnik, K. P., Yeh, J. T., and Pennline, H. W. (2004). Aqua ammonia process for simultaneous removal of CO₂, SO₂ and NO_x. International Journal of Environmental Technology and Management 4(1-2): 89-104.
- Riebesell, U., Wolf-Gladrow, D. A. and Smetacek, V. (1993). Carbon dioxide limitation of marine phytoplankton growth rates. Nature 361(249-251).
- Riemer, P. W. F. and Ormerod, W. G., (1995). International perspectives and the results of carbon dioxide capture disposal and utilisation studies. Energy Conversion and Management 36(6-9): 813-818.
- Rotatore, C., Colman, B., and Kuzma, M. (1995). The active uptake of carbon dioxide by the marine diatoms *Phaeodactylum tricorutum* and *Cyclotella sp.* Plant Cell Environment 18: 913-918.
- Rotatore, C., et al. (1992). Active uptake of CO₂ during photosynthesis in the green alga *Eremosphaera viridis* is mediated by a CO₂-ATPase. Planta 188(4): 539-545.
- Ryu, H. J., et al. (2009). Optimization of the influential factors for the improvement of CO₂ utilization efficiency and CO₂ mass transfer rate. Journal of Industrial and Engineering Chemistry 15(4): 471-475.
- Sarthou, G., Timmermans, K. R., Blain, S., and Treguer, P. (2005). Growth physiology and fate of diatoms in the ocean: a review. Journal of Sea Research 53: 25-42.
- Shimizu, T., et al. (1999). A Twin Fluid-Bed Reactor for removal of CO₂ from combustion processes. International Chemical Engineering 77: 62-70.

- Skjanes, K., et al. (2007). BioCO₂ - A multidisciplinary, biological approach using solar energy to capture CO₂ while producing H₂ and high value products. Biomolecular Engineering 24(4): 405-413.
- Sydney, E. B., et al. (2010). Potential carbon dioxide fixation by industrially important microalgae. Bioresource Technology 101(15): 5892-5896.
- Teramoto, M., K. Nakai, N. Ohnishi, Q Huang, T. Watari, and H. Matsuyama. (1996). Facilitated transport of carbon dioxide through supported liquid membranes of aqueous amine solutions. Industrial and Engineering Chemistry Research 35: 538-545.
- Tortell, C. L. M. a. P. D. (2008). Bicarbonate transport and extracellular carbonic anhydrase in marine diatoms. Physiologia Plantarum 133: 110-116.
- UOP. (2000). Benfield process. [Online]. Available from: www.uop.com/objects/99%20Benfield.pdf [2010, April 17]
- Van der Sluijs, J. O., Hendriks, C. A., and Blok, K. (1992). Feasibility of polymer membranes for carbon dioxide recovery from flue gases. Energy Conversion and Management 33(5-8): 429-436.
- Wang, J., Anthony, E. J., and Anabades, J. C. (2004). Clean and efficient use of petroleum coke for combustion and power regeneration. Fuel (83): 1341-1348.
- Williams, T. G. a. T., D. H. (1987). The role of external carbonic anhydrase in inorganic carbon acquisition by *Chlamydomonas reinhardtii* at alkaline pH. Plant Physiology 83(92-6).
- Xiang-xiang Wang, et al. (2008). The comparison of pKa determination between carbonic acid and formic acid and its application to prediction of the hydration numbers. Chemical Physics Letters 460(1-3): 339-342
- Yeh, A. C. and H. Bai (1999). Comparison of ammonia and monoethanolamine solvents to reduce CO₂ greenhouse gas emissions. The Science of The Total Environment 228(2-3): 121-133.
- Yeung , S. Y., Sun, B. K., Jong, M. P., Choong-II, L., and Yang, J. W. (1997). Carbon Dioxide Fixation by Algal Cultivation Using Wastewater Nutrients. Journal of Chemical and Biotechnology Technology 69: 451-455.
- Yokoyama, T. (2003). Greenhouse Gas Control Technologies. 6th International Conference on Greenhouse Gas Control Technologies (GHGT-6), Kyoto, Japan, Elsevier Science Ltd, Oxford, UK.

You, J. K., Jong Kyun You., and Won Hi Hong. (2008). Characteristics of CO₂ Absorption into Aqueous Ammonia. Separation Science and Technology 43: 766-777.



ศูนย์วิทยทรัพยากร
จุฬาลงกรณ์มหาวิทยาลัย



APPENDICES

ศูนย์วิทยทรัพยากร
จุฬาลงกรณ์มหาวิทยาลัย

APPENDIX A

TOTAL INORGANIC CARBON ANALYSE

EXPERIMENTAL DATA

Table A-1 %CO₂ dissolution efficiencies at different time at different pH value 6, 8 and 10 in 1 m high bubble column

(a) At pH 6

Time (min)	Total Inorganic Carbon (mg·L ⁻¹)			
	1 st time	2 nd time	SD	Avg
15	47.31	56.05	4.54	44.10
30	74.49	91.70	6.72	79.24
45	102.37	130.64	6.31	106.83
60	130.77	157.44	1.75	129.53

(b) pH 8

Time (min)	Total Inorganic Carbon (mg·L ⁻¹)			
	1 st time	2 nd time	SD	Avg
15	56.05	88.21	21.09	70.97
30	91.70	100.10	4.29	94.74
45	130.64	143.90	7.73	136.11
60	157.44	168.50	6.17	161.81

(c) At pH 10

Time (min)	Total Inorganic Carbon ($\text{mg}\cdot\text{L}^{-1}$)			
	1 st time	2 nd time	SD	Avg
15	92.85	86.53	4.47	89.69
30	126.00	138.72	8.99	132.36
45	154.10	163.92	6.94	159.01
60	182.50	188.02	3.90	185.26

Table A-2 %CO₂ dissolution efficiencies at different time at different pH 6, 8 and 10 in 1 m high packed column

(a) At pH 6 (at top and middle of the column)

Time (min)	Total Inorganic Carbon ($\text{mg}\cdot\text{L}^{-1}$)			
	1 st time	2 nd time	SD	Avg
15	44.21	46.69	1.75	45.45
30	129.61	127.22	1.69	129.25
45	219.41	190.02	20.78	205.55
60	277.31	257.82	13.78	268.40

Time (min)	Total Inorganic Carbon ($\text{mg}\cdot\text{L}^{-1}$)			
	1 st time	2 nd time	SD	Avg
15	93.26	133.61	23.60	113.43
30	143.26	157.11	8.31	150.18
45	220.96	186.01	19.88	203.48
60	224.66	220.11	2.36	222.38

(b) At pH 8 (at top and middle of the column)

Time (min)	Total Inorganic Carbon ($\text{mg}\cdot\text{L}^{-1}$)			
	1 st time	2 nd time	SD	Avg
15	60.57	57.04	2.34	58.81
30	162.88	142.05	14.57	152.47
45	248.64	226.52	15.49	237.58
60	287.84	285.32	1.63	286.58

Time (min)	Total Inorganic Carbon ($\text{mg}\cdot\text{L}^{-1}$)			
	1 st time	2 nd time	SD	Avg
15	102.03	110.43	5.51	106.23
30	141.83	144.13	2.10	142.98
45	201.83	204.13	2.10	202.98
60	240.23	214.33	14.38	227.28

(c) At pH 10 (at top and middle of the column)

Time (min)	Total Inorganic Carbon ($\text{mg}\cdot\text{L}^{-1}$)			
	1 st time	2 nd time	SD	Avg
15	132.19	117.11	10.54	124.65
30	204.79	197.21	5.23	201.00
45	276.99	264.51	8.70	270.75
60	340.49	302.61	26.66	321.55

Time (min)	Total Inorganic Carbon ($\text{mg}\cdot\text{L}^{-1}$)			
	1 st time	2 nd time	SD	Avg
15	144.83	135.34	5.00	140.09
30	192.43	189.24	1.56	190.84
45	240.13	243.24	2.52	241.69
60	261.33	251.64	5.11	256.49

Table A-3 %CO₂ dissolution efficiencies at different time and height in 3 m high packed column

(a) At 1m

Time (min)	Total Inorganic Carbon ($\text{mg}\cdot\text{L}^{-1}$)			
	1 st time	2 nd time	SD	Avg
15	54.41	66.83	8.78	60.62
30	257.13	272.53	10.89	264.83
45	297.03	300.53	2.47	298.78
60	311.13	309.63	1.06	310.38

(b) At 2m

Time (min)	Total Inorganic Carbon ($\text{mg}\cdot\text{L}^{-1}$)			
	1 st time	2 nd time	SD	Avg
15	29.47	28.69	0.27	29.08
30	153.68	122.43	11.05	138.06
45	231.18	205.63	9.03	218.41
60	274.68	232.53	14.90	253.61

(c) At 3m

Time (min)	Total Inorganic Carbon ($\text{mg}\cdot\text{L}^{-1}$)			
	1 st time	2 nd time	SD	Avg
15	19.84	16.84	1.06	18.34
30	52.95	58.76	2.05	55.85
45	142.36	172.12	10.52	157.24
60	180.91	197.52	5.87	189.21

Table A-4 %CO₂ dissolution efficiencies at different time and flowrate in range 10-40 cc·min⁻¹ in 1 m high bubble column

(a) At 10 cc·min⁻¹

Time (min)	Total Inorganic Carbon ($\text{mg}\cdot\text{L}^{-1}$)			
	1 st time	2 nd time	SD	Avg
15	89.94	86.31	0.39	88.12
30	123.09	138.50	5.42	130.79
45	151.19	163.70	2.32	157.44
60	179.59	187.80	3.07	183.69

(b) At 20 cc·min⁻¹

Time (min)	Total Inorganic Carbon ($\text{mg}\cdot\text{L}^{-1}$)			
	1 st time	2 nd time	SD	Avg
15	33.02	36.89	2.73	34.96
30	76.20	66.69	6.73	71.45
45	124.49	135.99	8.13	130.24
60	142.69	147.49	3.39	145.09

(c) At 30 cc·min⁻¹

Time (min)	Total Inorganic Carbon (mg·L ⁻¹)			
	1 st time	2 nd time	SD	Avg
15	52.32	51.80	0.37	52.06
30	104.69	97.40	5.16	101.04
45	164.99	167.30	1.63	166.14
60	212.99	203.50	6.71	208.24

(d) At 40 cc·min⁻¹

Time (min)	Total Inorganic Carbon (mg·L ⁻¹)			
	1 st time	2 nd time	SD	Avg
15	67.00	67.66	0.47	67.33
30	149.33	149.80	0.33	149.57
45	194.79	177.10	12.51	185.94
60	233.09	203.60	20.85	218.34

Table A-5 (a) %CO₂ dissolution efficiencies at different time and flowrate in range 10-40 cc·min⁻¹ in 2 m high bubble column (Samples collected at 1 m position)

(a.1) At 10 cc/min

Time (min)	Total Inorganic Carbon (mg·L ⁻¹)			
	1 st time	2 nd time	SD	Avg
15	65.19	68.53	2.36	66.86
30	128.34	130.78	1.73	129.56
45	156.44	152.92	2.49	154.68
60	184.84	180.02	3.41	182.43

(a.2) At 20 cc·min⁻¹

Time (min)	Total Inorganic Carbon (mg·L ⁻¹)			
	1 st time	2 nd time	SD	Avg
15	48.61	43.35	3.72	45.98
30	124.18	130.13	4.21	127.15
45	157.29	160.88	2.54	159.08
60	186.94	194.05	5.03	190.49

(a.3) At 30 cc·min⁻¹

Time (min)	Total Inorganic Carbon (mg·L ⁻¹)			
	1 st time	2 nd time	SD	Avg
15	50.74	46.09	3.29	48.41
30	116.99	130.12	9.28	123.55
45	182.59	182.86	0.19	182.72
60	227.69	234.22	4.61	230.95

(a.4) At 40 cc·min⁻¹

Time (min)	Total Inorganic Carbon (mg·L ⁻¹)			
	1 st time	2 nd time	SD	Avg
15	74.75	74.91	0.11	74.83
30	124.95	132.78	5.54	128.87
45	189.15	175.68	9.53	182.42
60	268.85	259.42	6.67	264.14

Table A-5 (b) %CO₂ dissolution efficiencies at different time and flowrate in range 10-40 cc/min in 2 m high bubble column (Samples collected at 2 m position)

(b.1) At 10 cc·min⁻¹

Time (min)	Total Inorganic Carbon (mg·L ⁻¹)			
	1 st time	2 nd time	SD	Avg
15	9.08	8.53	0.39	8.81
30	48.39	40.72	5.42	44.55
45	102.64	105.92	2.32	104.28
60	135.68	140.02	3.07	137.85

(b.2) At 20 cc·min⁻¹

Time (min)	Total Inorganic Carbon (mg·L ⁻¹)			
	1 st time	2 nd time	SD	Avg
15	13.02	16.69	2.59	14.86
30	76.20	66.69	6.73	71.45
45	124.49	135.99	8.13	130.24
60	210.69	197.49	9.34	204.09

(b.3) At 30 cc·min⁻¹

Time (min)	Total Inorganic Carbon (mg·L ⁻¹)			
	1 st time	2 nd time	SD	Avg
15	42.32	41.80	0.37	42.06
30	144.69	137.40	5.16	141.04
45	174.79	167.10	5.44	170.94
60	233.09	213.60	13.78	223.34

(b.4) At 40 cc·min⁻¹

Time (min)	Total Inorganic Carbon (mg·L ⁻¹)			
	1 st time	2 nd time	SD	Avg
15	124.23	109.53	10.39	127.80
30	184.73	173.66	7.83	190.12
45	213.93	194.13	14.00	214.95
60	250.83	227.53	16.48	250.10

Table A-6 % CO₂ dissolution efficiencies at different time and salinity**(a) At 5 ppt salinity**

Time (min)	Total Inorganic Carbon (mg·L ⁻¹)			
	1 st time	2 nd time	SD	Avg
15	51.57	52.45	7.22	61.78
30	86.83	88.77	7.59	97.57
45	107.43	103.37	5.47	115.17
60	127.13	136.67	10.28	141.67

(b) At 10 ppt salinity

Time (min)	Total Inorganic Carbon (mg·L ⁻¹)			
	1 st time	2 nd time	SD	Avg
15	23.59	29.39	10.26	38.11
30	46.14	50.96	9.92	60.17
45	72.86	74.07	8.64	85.08
60	99.77	103.72	9.61	113.36

(c) At 30 ppt salinity

Time (min)	Total Inorganic Carbon ($\text{mg}\cdot\text{L}^{-1}$)			
	1 st time	2 nd time	SD	Avg
15	18.18	18.06	4.67	24.79
30	45.28	46.93	5.30	52.77
45	66.21	72.87	7.07	76.21
60	93.47	101.18	7.44	103.99

Table A-7 %CO₂ dissolution efficiencies at different time and recycle flowrate using C.C.C.

(a) At 1 LPM recycle flowrate

Time (min)	Total Inorganic Carbon ($\text{mg}\cdot\text{L}^{-1}$)			
	1 st time	2 nd time	SD	Avg
15	17.20	27.43	7.24	22.32
30	22.97	33.87	7.71	28.42
45	49.47	48.71	0.53	49.09
60	58.61	65.26	4.70	61.94

(b) At 2 LPM recycle flowrate

Time (min)	Total Inorganic Carbon ($\text{mg}\cdot\text{L}^{-1}$)			
	1 st time	2 nd time	SD	Avg
15	33.38	33.19	0.13	33.28
30	53.08	46.88	4.38	49.98
45	66.63	64.92	1.21	65.77
60	82.06	82.89	0.59	82.47

(c) At 3LPM recycle flowrate

Time (min)	Total Inorganic Carbon (mg·L ⁻¹)			
	1 st time	2 nd time	SD	Avg
15	12.92	12.51	0.29	12.72
30	23.35	30.84	5.30	27.10
45	37.87	38.69	0.58	38.28
60	55.02	54.43	0.42	54.73



ศูนย์วิทยทรัพยากร
จุฬาลงกรณ์มหาวิทยาลัย

APPENDIX B

CULTIVATION OF *C. VALGARIS* WITH BICARBONATE

EXPERIMENTAL DATA

Table B-1 *C. vulgaris* cell concentration at different time without pH adjustment and NaHCO₃ added (Blank test)

Time (h)	Cell concentration (10 ⁶ cells ml ⁻¹)			
	1 st time	2 nd time	SD	Avg
0	1	1	0.00	1
24	15	17	1.41	16
48	22	24	1.41	23
72	34	37	2.30	35
96	49	52	1.94	51
120	60	63	2.12	62
144	64	67	2.12	65

ศูนย์วิทยทรัพยากร
จุฬาลงกรณ์มหาวิทยาลัย

Table B-2 *C. vulgaris* cell concentration at different time and with 30 ppm NaHCO₃ added (initial pH = 6)

Time (h)	Cell concentration (10 ⁶ cells ml ⁻¹)			
	1 st time	2 nd time	SD	Avg
0	1	1	0.00	1
24	20	19	0.88	13
48	45	43	2.65	37
72	66	65	3.54	66
96	96	100	1.94	98
120	103	108	3.18	110
144	104	108	1.77	115

Table B-3 *C. vulgaris* cell concentration at different time and with 30 ppm NaHCO₃ added (initial pH = 7)

Time (h)	Cell concentration (10 ⁶ cells ml ⁻¹)			
	1 st time	2 nd time	SD	Avg
0	1	1	0.00	1
24	14	13	0.88	13.13
48	35	39	2.65	36.88
72	64	69	3.54	66
96	97	100	1.94	98.38
120	108	113	3.18	110.25
144	114	116	1.77	115

Table B-4 *C. vulgaris* cell concentration at different time and with 30 ppm NaHCO₃ added (initial pH = 8)

Time (h)	Cell concentration (10 ⁶ cells ml ⁻¹)			
	1 st time	2 nd time	SD	Avg
0	1	1	0.00	1
24	18	11	0.88	7
48	30	33	0.35	10
72	51	57	2.12	22
96	66	70	3.18	35
120	70	75	2.83	40
144	72	76	3.01	42

Table B-5 *C. vulgaris* cell concentration at different time and with 30 ppm NaHCO₃ added (initial pH = 9)

Time (h)	Cell concentration (10 ⁶ cells ml ⁻¹)			
	1 st time	2 nd time	SD	Avg
0	1	1	0.00	1
24	8	6	0.88	7
48	10	11	0.35	10
72	24	21	2.12	22
96	37	33	3.18	35
120	42	38	2.83	40
144	44	40	3.01	42

Table B-6 *C. vulgaris* cell concentration at different time and with 80 ppm NaHCO₃ added (initial pH = 7)

Time (h)	Cell concentration (10 ⁶ cells ml ⁻¹)			
	1 st time	2 nd time	SD	Avg
0	1	1	0.00	1
24	14	14	0.35	14
48	31	33	1.24	32
72	67	68	0.71	67
96	97	98	0.18	97
120	109	111	1.06	110
144	117	118	1.24	117

Table B-7 *C. vulgaris* cell concentration at different time and with 200 ppm NaHCO₃ added (initial pH = 7)

Time (h)	Cell concentration (10 ⁶ cells ml ⁻¹)			
	1 st time	2 nd time	SD	Avg
0	1	1	0.00	1
24	18	17	0.53	17
48	35	32	1.94	33
72	62	61	0.71	62
96	94	92	1.59	93
120	108	105	2.47	106
144	117	118	1.06	117

Table B-8 *C. vulgaris* cell concentration at different time and with CO₂ dissolution water (initial pH = 7)

Time (h)	Cell concentration (10 ⁶ cells ml ⁻¹)			
	1 st time	2 nd time	SD	Avg
0	1	1	0.00	1
24	13	13	0.18	13
48	51	50	1.24	50
72	76	80	3.01	78
96	103	104	0.88	103
120	120	121	0.88	121
144	124	124	0.00	124

ศูนย์วิทยทรัพยากร
จุฬาลงกรณ์มหาวิทยาลัย

APPENDIX C

SAMPLE CALCULATIONS

C.1 %Efficiency of CO₂ dissolution

% Efficiency can be calculated by using equation (3.2);

$$\%Efficiency = \frac{TIC \times V_L}{\left(\frac{PQ_g t M_w}{RT}\right)}$$

For example, experiment in section 4.1.3, sample collected at 2 m position in which: P = 1.3 bar, T = 298 K, TIC at 60 min = 253.60 mg·L⁻¹, Volume of liquid (V_L) = 1200 mL, CO₂ flowrate = 10 cc·min⁻¹. Substitute these variables and get %efficiency = 21.67%

C.2 Gas hold up

Gas hold up can be determined from equation (4.3) in Chapter 4:

$$\epsilon_g = \frac{V_g}{V}$$

V_g can be obtained from increasing in column's volume when CO₂ enter the system.

For 1 m high bubble column; Volume of liquid = 1500 mL and Volume of gas = 178 mL;
Substitute in equation (4.3) and obtain $\epsilon_{g,b} = 0.11$.

For 1 m high packed column; Volume of liquid = 1200 mL and Volume of gas = 270 mL;
Substitute in equation (4.3) and obtain $\epsilon_{g,p} = 0.23$.

C.3 Specific growth rate (μ)

Specific growth rate can be computed by equation (3.3) in Chapter 3:

$$\mu = \frac{\ln(N_2) - \ln(N_1)}{t_2 - t_1}$$

Plot $\ln(N_t)/\ln(N_0)$ vs. $(t-t_0)$ and obtain μ from slope of plotting

Where	N_t	=	Cell concentration at t time (10^6 cells ml^{-1})
	N_0	=	Cell concentration at the beginning (t_0) (10^6 cells ml^{-1})
	t	=	Sample collected time (h)
	t_0	=	Time at the beginning of cultivation (h)

It noted that only cell concentration in log phase will be used to calculate for μ . For example, cultivation of *C. vulgaris* at initial pH = 7 gave the $\mu = 0.045 \text{ h}^{-1}$ or 1.080 d^{-1} (Figure C.1)

ศูนย์วิทยทรัพยากร
จุฬาลงกรณ์มหาวิทยาลัย

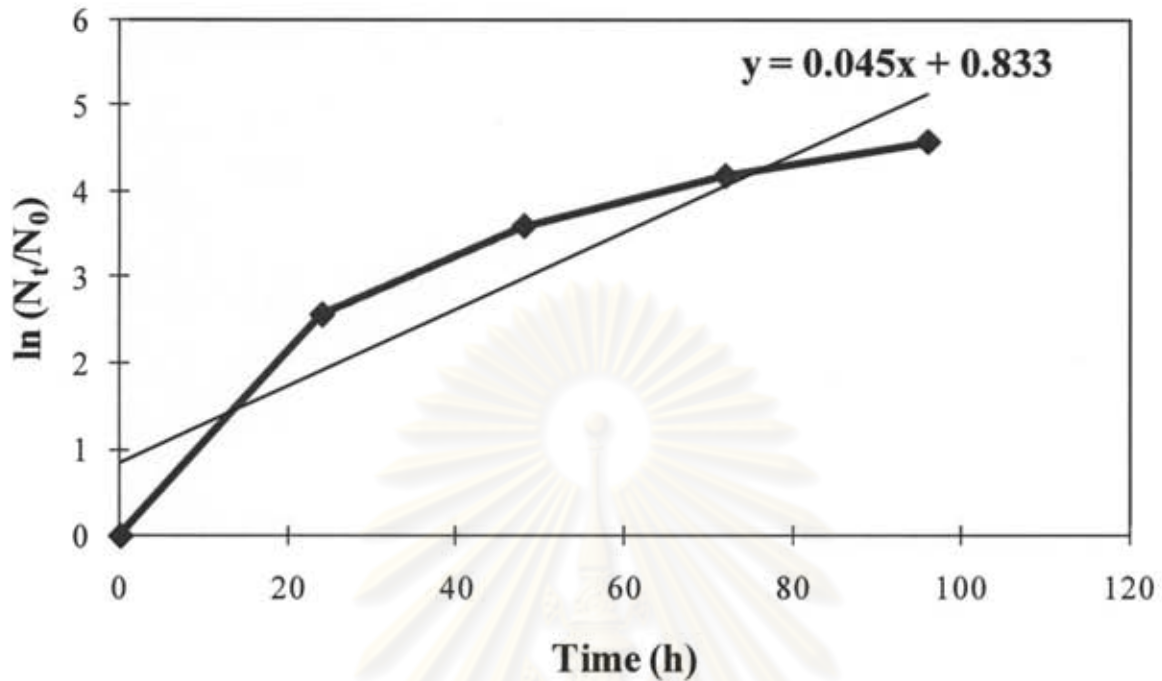


Figure C.1 Plot of $\ln(N_t/N_0)$ vs. Time (h): Determination of μ

C.4 Amount of Sodium Bicarbonate fed into the cultivation system

30 ppm ($\text{mg}\cdot\text{L}^{-1}$) of NaHCO_3 will need 30 mg for 1 L cultivation system

In case of 2.8 L cultivation system will need NaHCO_3 $2.8 \times 30 = 84$ mg to be dissolved.

ศูนย์วิทยทรัพยากร
จุฬาลงกรณ์มหาวิทยาลัย

APPENDIX D**PUBLICATIONS****International Symposium / Conference Proceedings**

Pichiansoontorn P. and Pavasant P., (2010). ACCELERATING MICROALGAL GROWTH WITH CO₂ TRANSFORMATION. 17th Regional Symposiums on Chemical Engineering (RSCE) Conference Book of Abstract, pp.150, November 22nd-23rd, Bangkok, Thailand

National Symposium / Conference Proceedings

Pichiansoontorn P. and Pavasant P., (2010) Combined Effects of Design and pH-shift for CO₂ absorption in bubble columns. Climate Thailand Conference 2010 proceeding, pp. 567-572, August 19th-20th, Bangkok, Thailand



ศูนย์วิทยทรัพยากร
จุฬาลงกรณ์มหาวิทยาลัย

BIOGRAPHY

Name : Yossaran Pichiansoontorn
Date of Birth : January 10, 1987
Place of Birth : Bangkok, Thailand
Institution Attended : Suankularb Wittayalai School, Bangkok, Thailand

Certificate of Mathayomsuksa 6

Department of Chemical Technology,
Faculty of Science, Chulalongkorn University,
Bangkok, Thailand

B.Sc. Chemical Engineering

In 2009, He continued his further study for Master's degree in Chemical Engineering at Department of Chemical Engineering, Faculty of Engineering, Chulalongkorn University. He participated in Environmental and Safety Research Group.



ศูนย์วิทยทรัพยากร
จุฬาลงกรณ์มหาวิทยาลัย